FAULT TRACE MAPPING AND SURFACE-FAULT-RUPTURE SPECIAL STUDY ZONE DELINEATION OF QUATERNARY-ACTIVE FAULTS IN CENTRAL UTAH, GARFIELD, JUAB, MILLARD, PIUTE, SANPETE, AND SEVIER COUNTIES, UTAH

by Adam I. Hiscock, Tyler R. Knudsen, and Rachel N. Adam

REPORT OF INVESTIGATION 293
UTAH GEOLOGICAL SURVEY
UTAH DEPARTMENT OF NATURAL RESOURCES
2025

Blank pages are intentional for printing purposes.

FAULT TRACE MAPPING AND SURFACE-FAULT-RUPTURE SPECIAL STUDY ZONE DELINEATION OF QUATERNARY-ACTIVE FAULTS IN CENTRAL UTAH, GARFIELD, JUAB, MILLARD, PIUTE, SANPETE, AND SEVIER COUNTIES, UTAH

by Adam I. Hiscock, Tyler R. Knudsen, and Rachel N. Adam

Cover photo: *View looking southeast towards the Sevier fault and Glenwood Mountain, Sevier County, Utah.*

Suggested citation:

Hiscock, A.I., Knudsen, T.R., and Adam, R.N., 2025, Fault trace mapping and surface-fault-rupture special study zone delineation of quaternary-active faults in central Utah, Garfield, Juab, Millard, Piute, Sanpete, and Sevier Counties, Utah: Utah Geological Survey Report of Investigation 293, 26 p., https://doi.org/10.34191/RI-293.

UTAH DNR GEOLOGICAL SURVEY

REPORT OF INVESTIGATION 293
UTAH GEOLOGICAL SURVEY
UTAH DEPARTMENT OF NATURAL RESOURCES
2025

STATE OF UTAH
Spencer J. Cox, Governor

DEPARTMENT OF NATURAL RESOURCES
Joel Ferry, Executive Director

UTAH GEOLOGICAL SURVEY
Darlene Batatian, Director

PUBLICATIONS
contact
Natural Resources Map & Bookstore
1594 W. North Temple
Salt Lake City, UT 84116
telephone: 801-537-3320
toll-free: 1-888-UTAH MAP
website: utahmapstore.com
email: geostore@utah.gov

UTAH GEOLOGICAL SURVEY
contact
1594 W. North Temple, Suite 3110
Salt Lake City, UT 84116
telephone: 801-537-3300
website: geology.utah.gov

This material is based on work supported by the U.S. Geological Survey under grant no. G24AP00313. The views and conclusions contained in this document are those of the authors and should not be interpreted as necessarily representing the opinions or official policies, either expressed or implied, of the U.S. Government. Any use of trade, product, or firm names is for descriptive purposes only and does not imply endorsement by the U.S. Government.

CONTENTS

FIGURES

TABLE

GIS DATA

https://ugspub.nr.utah.gov/publications/reports_of_investigations/ri-293/ri-293.zip

FAULT TRACE MAPPING AND SURFACE-FAULT-RUPTURE SPECIAL STUDY ZONE DELINEATION OF QUATERNARY-ACTIVE FAULTS IN CENTRAL UTAH, GARFIELD, JUAB, MILLARD, PIUTE, SANPETE, AND SEVIER COUNTIES, UTAH

by Adam I. Hiscock, Tyler R. Knudsen, and Rachel N. Adam

ABSTRACT

The central Utah region contains numerous large, hazardous faults which pose significant earthquake risk. Faults in this region define the seismically active transition zone between the Colorado Plateau and Basin and Range physiographic provinces. This zone of active seismicity, referred to as the Intermountain Seismic Belt (ISB), poses a significant earthquake risk to growing populations and critical infrastructure. Utah's largest recorded historical earthquake, the 1901 M6.6 Tushar Mountains earthquake (Arabasz et al., 2017), occurred in the study area. The area of this study is one of the fastest growing rural regions of Utah and includes many critical infrastructure hubs and corridors.

Airborne light detection and ranging (lidar) elevation data were collected in central Utah in 2016, 2018, and 2020. High-resolution topographic data derived from these lidar datasets have allowed for a complete update of the mapping of surface traces of faults in the area. Previously, the surface location and extent of fault traces in the region were not well understood, owing to limited aerial photography coverage, heavy vegetation near range fronts, and the difficulty in recognizing moderate (<1 m) scarp heights in the field or on aerial photographs. In addition to lidar-derived elevation data, other datasets including historical aerial photography, previous geologic mapping, limited paleoseismic investigations, and field investigations were used to identify and map surface fault traces and infer fault locations. Specific faults mapped as part of this investigation include (from north to south): Sage Valley faults, Little Valley faults, Scipio Valley faults, Japanese and Cal Valley faults, Pavant Range fault, Maple Grove faults, Red Canyon fault scarps, Elsinore fault, Sevier fault, Annabella Graben faults, Joseph Flats area faults and syncline, Dry Wash fault and syncline, Marysvale-Circleville area faults, and Tushar Mountains (East Side) fault (all names from the *Utah Geologic Hazards Portal*, https://hazards.geology.utah.gov/).

We delineated recommended special-study zones around mapped fault traces to facilitate understanding of the surface-rupturing hazard and associated risk. The fault geometries, attributes, and special-study zones were published in the *Utah Geologic Hazards Portal* simultaneously with this Report of Investigation and are also included with this report as a GIS database. Defining surface-fault-rupture special-study zones encourages the creation and implementation of municipal and county geologic-hazard ordinances dealing with hazardous faults. We also identified potential paleoseismic investigation sites where fault scarps appear relatively pristine, are in geologically favorable settings, and where additional earthquake timing data would be beneficial to earthquake research of regional faults in central Utah. This report contains supplementary material describing the data and methods used to perform the mapping and locating potential paleoseismic investigation sites. This work is critical to raise awareness of earthquake hazards in areas of Utah experiencing rapid growth.

INTRODUCTION AND PURPOSE

Central Utah has many Quaternary-active normal faults which pose a significant earthquake hazard to the growing Sevier Valley area (Figure 1) and infrastructure corridors that include major power transmission lines, telecommunications cables, and the Kern River natural gas transmission line that are critical for the economic and societal well-being of the state of Utah. The Sevier Valley is a major rural regional population center that is crossed by north-south (U.S. Highway 89) and east-west (U.S. Interstate 70 and U.S. Highway 50) transportation corridors (Figure 1). Additionally, U.S. Interstate 15 overlies numerous faults in the Scipio Valley area. The State of Utah projects that Sevier County will grow 54% by 2065, and that Sanpete County will grow 70% by 2065 (Perlich et al., 2017). Communities such as Richfield, Elsinore, Monroe, Salina, and Gunnison constitute most of the population in Sevier County and are directly adjacent to several fault zones in the area, including the Sevier fault zone (Figure 1). In addition, the area has several popular state parks and reservoirs, such as Fremont Indian State Park and Museum, Yuba State Park and reservoir, and Piute State Park and reservoir. In addition to strong ground shaking, numerous potentially damaging earthquake-triggered rockfalls along steep range fronts and liquefaction hazard along lowlands adjacent to water bodies can also be expected in these areas during earthquakes. The dams and dikes of regional reservoirs, such as Yuba and Piute, are also particularly vulnerable to large earthquakes. Both Piute (Piute State Park) and Sevier Bridge (Yuba State Park) dams are listed as high-hazard dams by the

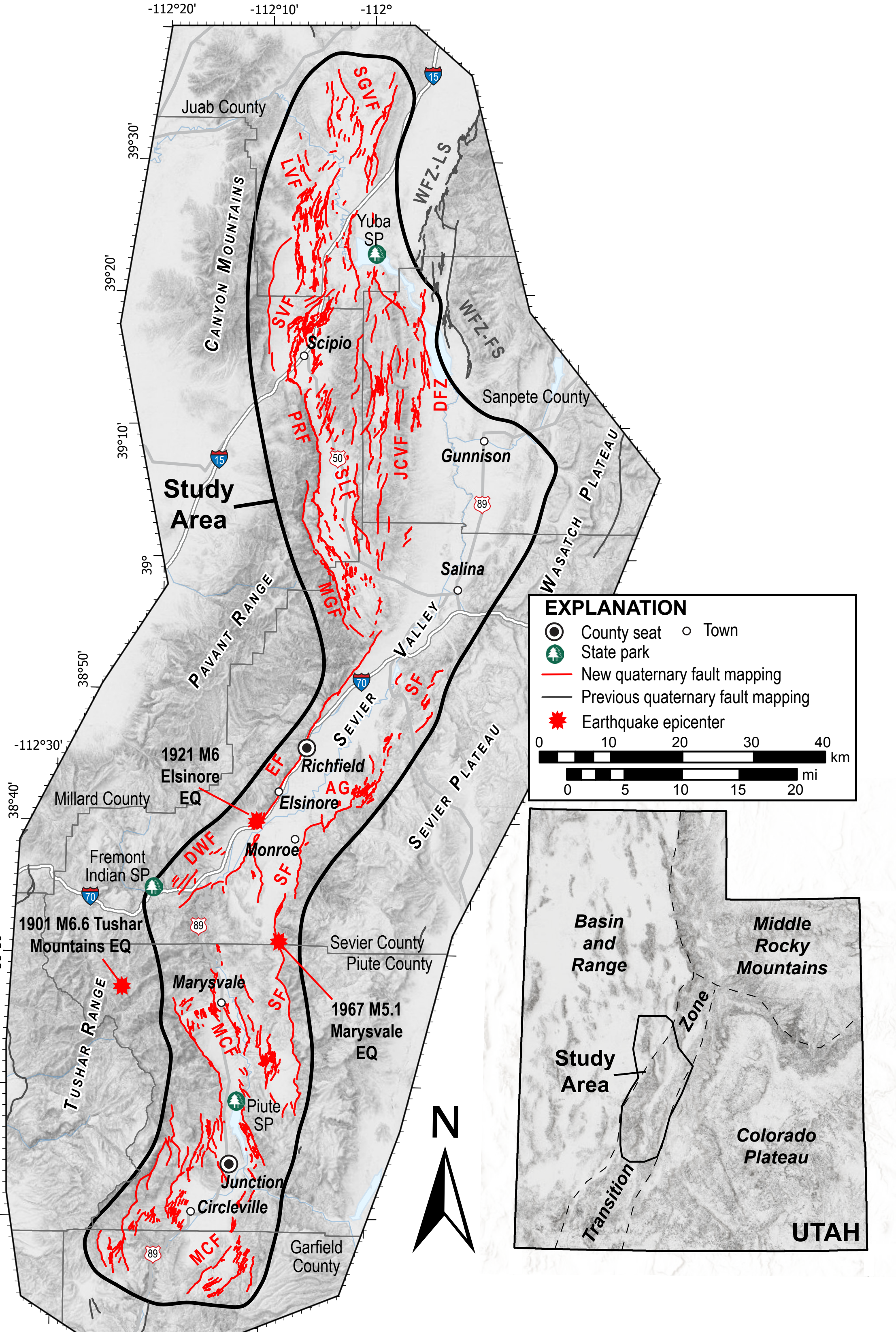

Figure 1. Fault zones mapped as part of this study (SGVF = Sage Valley faults, LVF = Little Valley faults, SVF = Scipio Valley faults, PRF = Pavant Range fault, MGF = Maple Grove fault, SLF = Scipio Lake faults, DFZ = Dover fault zone, EF = Elsinore fault, SF = Sevier fault, AG = Annabella graben, DWF = Dry Wash fault, MCF = Marysvale –Circleville area faults), other regional faults from the Utah Geologic Hazards Portal (undated; WFZ-LS = Wasatch fault zone–Levan segment, WFZ-FS = Wasatch fault zone–Fayette segment), cities, significant earthquake epicenters (Arabasz et al., 2017), study area, and other physical features. Inset map of Utah in bottom right shows the study area boundary and geological provinces. Shaded relief base maps generated from ESRI, USGS, and NOAA elevation data.

Utah Division of Water Resources Dam Safety Program due to significant population and infrastructure in the pathway of dam-breach flooding. Also housed in the area is the State of Utah Division of Technology Services Richfield Data Center, which serves as the primary backup data center for all state government IT services.

Previous studies in the central Utah area have provided valuable mapping of the extent of faults in the region (Anderson and Bucknam, 1979, Bucknam and Anderson, 1979). However, no detailed fault scarp mapping (better than 1:100,000 scale) or surface-fault-rupture special-study-zone delineation was completed for any of the Quaternary-active faults mapped in the region. Various geologic quadrangle maps at 1:24,000 and 1:100,000 scale cover a large part of the area, but were created using limited available aerial photography, topographic maps, and fieldwork. On these maps, fault scarps were poorly defined owing to a general lack of study and difficulty in recognizing small to moderate (<1 m high) scarps in the field or on aerial photographs. These mapping limitations contributed to the scarcity of detailed paleoseismic-trenching investigations and earthquake timing data in the area.

Recently acquired airborne light detection and ranging (lidar) data for central Utah has allowed us to create accurate, detailed maps of faults in the area. Lidar has greatly improved our abilities to identify and map surficial fault traces in areas of active, young, faulting. The ability to create sub-meter resolution, bare-earth elevation models without vegetation can reveal subtle patterns created by geologic processes, including fault zones (Meigs, 2013). Lidar datasets for central Utah were collected in 2016, 2018, and 2020 (Utah Geospatial Reference Center, 2016, 2018, and 2020) by the State of Utah, the Utah Geological Survey (UGS), and its partners (Utah Division of Emergency Management, Federal Emergency Management Agency [FEMA], USGS, Natural Resources Conservation Service, National Park Service, U.S. Forest Service, and others). These lidar datasets also allow for identification of sites suitable for future paleoseismic investigations.

In 2024, the UGS received matching funds from the USGS Earthquake Hazards Program, External Grants Program (grant no. G24AP00313) for this project. This UGS Report of Investigation publication fulfills the publishing requirements for the USGS External Grants Program funding. The results of this investigation will help reduce losses from future earthquakes by permitting more accurate regional earthquake-hazard evaluations. Complete fault geometries, attributes, and surface-fault-rupture special-study zones of central Utah faults from this study were published in the UGS's online *Utah Geologic Hazards Portal* (https://hazards.geology.utah.gov/, Utah Geological Survey [undated]). Additionally, fault geometries and attributes were submitted to the USGS for inclusion in the *Quaternary Fault and Fold Database of the United States*. The data in the UGS's hazards portal database represents the most up-to-date fault geometries of central Utah faults and will continue to be updated in the future. In addition, a fully-attributed geodatabase containing fault geometries and surface-fault-rupture special-study zones is included as a stand-alone product with this report. These map products characterize surface-faulting hazard and associated risks and are critical to the creation, implementation, and enforcement of local government geologic-hazard ordinances in jurisdictions containing hazardous faults. This project is part of an ongoing effort by the UGS to map and characterize hazardous Quaternary faults in urban and rural areas (Hiscock and Hylland, 2015; McDonald et al., 2020; Hiscock et al., 2021; Knudsen et al., 2021; Hiscock et al., 2024). The results from this study will be presented and shared with local governments, professional organizations, and the general public in Utah. This work is essential to adequately characterize the seismic hazard and to mitigate earthquake risk to vulnerable communities and infrastructure in central Utah.

The purpose of this study was to map fault traces at a scale of 1:10,000 using the new lidar elevation data, identify previously unmapped surface fault traces, determine approximate fault age categories from geomorphic relationships and previous geologic mapping, define special-study zones, and identify potential sites for future paleoseismic investigations of active faults in central Utah (Table 1). Numerous large, Quaternary-active normal faults cut the central Utah region. For this study, we focused on mapping the following fault zones (from north to south: Sage Valley faults, Little Valley faults, Scipio Valley faults, Japanese and Cal Valley faults, Pavant Range fault, Maple Grove faults, Red Canyon fault scarps, Elsinore fault, Sevier fault, Annabella Graben faults, Joseph Flats area faults and syncline, Dry Wash fault and syncline, Marysvale-Circleville area faults, and Tushar Mountains (East Side) fault (all names from the *Utah Geologic Hazards Portal*).

BACKGROUND

Geologic Setting

Quaternary-active normal faults in central Utah lie within the structural transition zone between the actively extending Basin and Range Province to the west, the quasi-stable Colorado Plateau Province to the east, and the gradually uplifting Middle Rocky Mountains Province to the northeast (Figure 2; Stokes, 1977, 1986; Anderson and Barnhard, 1992; Wannamaker et al., 2001). This transition zone possesses a mix of characteristics from both the extensional Basin and Range Province and the stable Colorado Plateau, encompassing a broad area of distributed deformation where the extensional block faulting of the Basin and Range is cutting into, or overprinting, the much more tectonically stable westernmost Colorado Plateau (Wannamaker et al., 2001). This transition from a stable continental platform (the Colorado Plateau) to the tectonically active extension of the Basin and Range is very complex, with likely interplay between active tectonic forces and inherited geological structures, such as

Table 1. *Potential paleoseismic sites in the Central Utah region.*

Site Number	Fault Zone/Name	Comments	NAD83 UTM Zone 12N	
			UTM Easting	UTM Northing
AG-1	Annabella Graben	Best location for a long trench to encompass all the fault scarps associated with the Annabella Graben.	410956	4284653
AG-2	Annabella Graben	Second-best location for a long trench to encompass all the fault scarps associated with the Annabella Graben.	411249	4284960
AG-3	Annabella Graben	Decent scarp on Late Pleistocene alluvium. Would need either two trenches (combined with AG-4) or a long trench to capture full fault history.	412192	4284574
AG-4	Annabella Graben	Decent scarp on Late Pleistocene alluvium. Would need either two trenches (combined with AG-3) or a long trench to capture full fault history.	412344	4284524
DFZ-1	Dover FZ	Young small scarp cutting young fan.	420847	4348083
DFZ-2	Dover FZ	Closer to older pediment surface, but still good scarp on young fan.	420841	4347950
DFZ-3	Dover FZ	Young scarp in mouth of drainage.	420386	4350759
EF-1	Elsinore fault	Great scarp on young Holocene allvium. Fault is very short and only appears to cut young alluvium in the mouth of this one drainage.	407164	4297205
JCVF-1	Japanese and Cal Valleys faults	Nice scarp formed on likely Late Pleistocene fan. Ideally, fault to east would also be trenched (site JVF-2).	417150	4338553
JCVF-2	Japanese and Cal Valleys faults	Nice scarp formed on likely Late Pleistocene fan. Ideally, fault to west would also be trenched (site JVF-1). Slight chance scarp is bedrock-cored.	417567	4338786
JCVF-3	Japanese and Cal Valleys faults	Appears to be the only scarp formed on alluvium along the fault bounding the west side of the Japanese Valley graben. Might be bedrock-cored.	413416	4331707
JCVF-4	Japanese and Cal Valleys faults	Good scarp representative of many enigmatic intrabasin scarps formed on Late Pleistocene to Holocene alluvial-fan deposits in central Japanese Valley.	414097	4340944
LVF-1	Little Valley faults	Relatively young, well-preserved scarp formed on Late Pleistocene to Holocene alluvium.	405550	4369296
LVF-2	Little Valley faults	Relatively young, well-preserved scarp formed on Late Pleistocene to Holocene alluvium. One of the more prominent faults in the Little Valley fault complex.	406255	4368346
LVF-3	Little Valley faults	Relatively young, well-preserved scarp formed on Late Pleistocene to Holocene alluvium. One of the more prominent faults in the Little Valley fault complex.	407314	4367005
LVF-4	Little Valley faults	Suitable scarp formed on Late Pleistocene alluvial fan.	403181	4361930
MGF-1	Maple Grove faults	Trench can extend across two Holocene faults at base of range front.	405506	4325886
MGF-2	Maple Grove faults	Holocene fault scarp located on a preserved fan surface along the range front.	405530	4325081
MGF-3	Maple Grove faults	Good expression of Pleistocene fault along eastern range front into Quaternary deposits.	411746	4325887
MGF-4	Maple Grove faults	Topographic inflection along eastern rangefront on an abandoned channel into Quaternary deposits.	411616	4321626
MGF-5	Maple Grove faults	Holocene fault scarp located on a preserved fan surface along the range front.	407490	4315697
MGF-6	Maple Grove faults	Holocene fault scarp located on a preserved fan surface along the range front.	408553	4314013
MGF-7	Maple Grove faults	Holocene fault scarp located on a preserved fan surface along the range front.	409437	4310848
SFZ-1	Sevier fault zone	Good scarp on small section of cut-off alluvial fan. Slight potential for shallow bedrock.	408730	4281842
SFZ-10	Sevier fault zone	Decent, slightly degraded, scarp in young Holocene alluvium.	414758	4286735
SFZ-11	Sevier fault zone	Good scarp on a short fault cutting young Holocene alluvium.	417450	4292617
SFZ-12	Sevier fault zone	Good scarp on a short fault cutting young Holocene alluvium.	417554	4292748
SFZ-2	Sevier fault zone	Nice scarp, but high potential for shallow bedrock.	409552	4282161
SFZ-3	Sevier fault zone	Possible site on a cut-off section of fan. Older fan than site directly south of here (site SFZ-4).	410668	4282713
SFZ-4	Sevier fault zone	Small piece of youngest fan, good site if large enough surface for a trench.	410658	4282634
SFZ-5	Sevier fault zone	Young scarps in active drainage. Multiple good trench sites along here (although in a massive landslide complex).	407490	4280005
SFZ-6	Sevier fault zone	Good scarp all through here, multiple good trench sites. Young fan/drainage, may be fluvial modification.	407590	4280276
SFZ-7	Sevier fault zone	Good young scarp, could trench anywhere along here.	414022	4285003
SFZ-8	Sevier fault zone	Good scarp cutting young alluvium in the mouth of an active drainage.	403299	4241879
SFZ-9	Sevier fault zone	Possible site in mouth of drainage, but would need better field checking to ensure suitability for a paleoseismic trench.	403446	4242267
SGVF-1	Sage Valley faults	Suitable scarp formed on Late Pleistocene alluvial fan. This appears to be the best trench site on the Sage Valley fault.	413939	4374447
SGVF-2	Sage Valley faults	Suitable scarp formed on Late Pleistocene alluvial/lacustrine deposits. Scarp is on the second-most significant fault in the Sage Valley area.	411348	4374027
SVF-1	Scipio Valley faults	Likely Holocene scarp formed on alluvium.	405383	4352410
SVF-2	Scipio Valley faults	Holocene scarp formed on alluvium. Suitable trench site on one of the most prominent faults in Scipio Valley.	401948	4348136
SVF-3	Scipio Valley faults	Holocene scarp formed on alluvium. Scarp is on west-bounding fault of prominent graben. Would want to combine with SVF-4 on east side of graben.	402368	4344599
SVF-4	Scipio Valley faults	Holocene scarp formed on alluvium. Scarp is on east-bounding fault of prominent graben. Would want to combine with SVF-3 on west side of graben.	402818	4344385
SVF-5	Scipio Valley faults	Suitable scarp formed on Late Pleistocene alluvial fan. This appears to be the best trench site for the significant fault bounding the northeast side of Scipio Valley.	407126	4350196
SVF-6	Scipio Valley faults	Suitable scarp formed on Late Pleistocene alluvial fan. Scarp formed on prominent fault immediately east of the town of Scipio.	405553	4344957
SVF-7	Scipio Valley faults	Holocene scarp formed on alluvium. This is an alternative site to SVF-3.	401801	4342893
SVMCF-1	Sevier Valley-Marysvale-Circleville area faults	Young scarp near mouth of drainage, could have even younger alluvium burying base of scarp.	385084	4227813
SVMCF-10	Sevier Valley-Marysvale-Circleville area faults	Decent scarp on Late Pleistocene alluvial fan. Combine with SVMCF-11 as a multiple trench study for more paleoseismic data.	400116	4246554
SVMCF-11	Sevier Valley-Marysvale-Circleville area faults	Decent scarp on Late Pleistocene alluvial fan. Combine with SVMCF-10 as a multiple trench study for more paleoseismic data.	399877	4246885
SVMCF-12	Sevier Valley-Marysvale-Circleville area faults	Ok scarp on Late Pleistocene fan. Field checking would be essential to ensure no human modification to scarp before trenching.	399385	4249172
SVMCF-13	Sevier Valley-Marysvale-Circleville area faults	Good scarp, base likely buried by Holocene alluvium, but could be suitable for trenching.	399003	4249511
SVMCF-2	Sevier Valley-Marysvale-Circleville area faults	Good scarp, but strong possibility of shallow bedrock here.	384824	4226793
SVMCF-3	Sevier Valley-Marysvale-Circleville area faults	Small subtle fault cutting young alluvium. Would need multiple trenches to get full paleoseismic history.	385659	4226976
SVMCF-4	Sevier Valley-Marysvale-Circleville area faults	Small subtle fault cutting young alluvium. Would need multiple trenches to get full paleoseismic history.	386004	4226803
SVMCF-5	Sevier Valley-Marysvale-Circleville area faults	Large scarp cutting young alluvium, good site.	386434	4230865
SVMCF-6	Sevier Valley-Marysvale-Circleville area faults	Nice graben with several suitable trench sites to the south of this location. Part of distributed faulting so multiple trenches would be necessary.	395010	4220820
SVMCF-7	Sevier Valley-Marysvale-Circleville area faults	Nice graben suitable for trenching. Part of distributed faulting so multiple trenches would be necessary.	394975	4220645
SVMCF-8	Sevier Valley-Marysvale-Circleville area faults	Great scarp cutting Late Pleistocene fan. Slight potential for shallow bedrock. Part of distributed faulting, so multiple trenches would be necessary.	390685	4235215
SVMCF-9	Sevier Valley-Marysvale-Circleville area faults	Good small scarp cutting Late Pleistocene fan. Could trench anywhere along here. Part of distributed faulting, so multiple trenches would be necessary.	391404	4235710

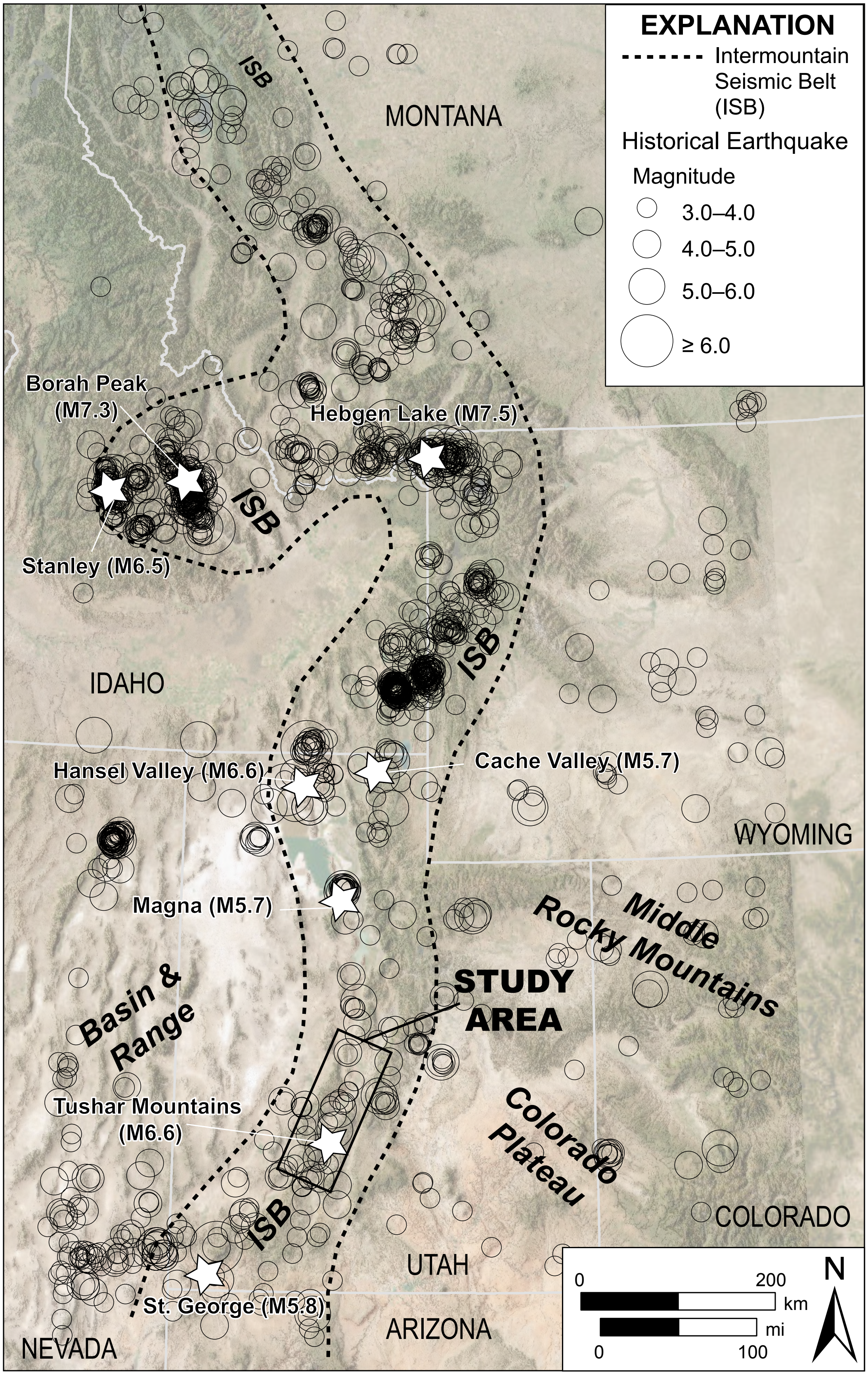

Figure 2. Map showing the Intermountain Seismic Belt (ISB) and other geographical provinces. Selected historical large earthquakes in the ISB are shown as white stars, other earthquakes shown as circles corresponding to magnitude. Data from U.S. Geological Survey (undated[b]). Central Utah region highlighted with black box titled study area.

the Yavapai and Mojave terranes (Wannamaker et al., 2001). The northern part of the transition zone is narrow, with most of the extension accommodated along the Wasatch fault zone, whereas in southwestern Utah, the transition zone is much wider (~60 mi [100 km]) and encompasses multiple fault zones (Wannamaker et al., 2001).

Central Utah lies within the southern to middle part of the Intermountain Seismic Belt (ISB)—a north-south-trending zone of pronounced seismicity that extends from Montana to southeastern Nevada and northwestern Arizona (Figure 2; Smith and Sbar, 1974). This zone is generally considered the most seismically active area of Utah (Anderson and Barnhard, 1992). Central Utah has a record of seismicity that includes the largest magnitude (M) earthquake ever recorded in the state of Utah, the 1901 M6.6 Tushar Mountains earthquake (Arabasz et al., 2017) (Figures 1 and 2). This earthquake was felt over a wide area and, despite no reported loss of life, caused widespread damage to communities in the Sevier Valley (University of Utah Seismograph Stations, 2020a). The 1921 Elsinore earthquake sequence produced a mainshock of M6.0, with aftershocks of M5.7 and 6.0, also caused widespread building damage to communities in the Sevier Valley (University of Utah Seismograph Stations, 2020b). The 1967 M5.1 Marysvale earthquake was also felt throughout the region and caused minor damage to communities (Arabasz et al., 2017) (Figure 1). Although a large surface-rupturing earthquake (> ~M6.5) has not occurred historically in the region, scarps formed on young alluvial-fan deposits provide evidence that such large earthquakes have occurred in the past.

Previous Work and Geologic Mapping

Anderson and Bucknam (1979) and Bucknam and Anderson (1979) conducted the first fault scarp mapping on the Richfield and Delta 30′ x 60′ quadrangles. The quality and detail of their mapping is low (1:100,000 scale) and the mapping relied on 1:20,000 air photos and limited field mapping. Rowley et al. (2002) produced a map focused on the deposits associated with the Marysvale Volcanic Field and identified several fault scarps on unconsolidated sediments but did not map these scarps in great detail. Oviatt (1992) discovered dozens of previously unmapped faults while mapping the Quaternary geology of the Scipio-Round Valley region and hypothesized their ages.

Numerous bedrock and surficial geologic mapping studies have been conducted in the central Utah region. Geologic quadrangle mapping at 1:24,000-scale covers parts of the Sevier fault (Steven, 1979; Rowley et al., 1979b, 1981a, 1981b, 1988a, 1988b; Anderson and Rowley, 1986); Marysvale-Circleville area faults (Anderson, 1986; Anderson and Rowley, 1986; Anderson et al., 1990; Cunningham et al., 1983; Rowley et al., 1979b, 1988a, 1988b, 2002); Elsinore fault (Steven, 1979; Willis, 1988, 1994); Red Canyon, Maple Grove, and Pavant Range faults (Hintze, 1991a, 1991b); Scipio and Little Valley faults (Hintze, 1991b, 1991c, 1991d; 1991e; Michaels, 1994; Oviatt and Hintze, 2005); Sage Valley faults (Clark, 1990, 2003; Oviatt and Hintze, 2005; Felger et al., 2007); Japanese and Cal Valley faults (Hintze, 1991b; Willis, 1991; Peterson, 1997); and Dover fault zone (Peterson, 1997; Willis, 1991). These previous mapping studies relied on limited available aerial photography and lacked the advantage of detailed lidar-derived elevation products. Geologic mapping at 1:100,000 scale has been completed for most of the project area (Hintze and Davis, 2002; Rowley et al., 2005; Witkind et al., 2007; Hintze et al., 2008). The most recent intermediate scale mapping is being completed with the advantage of lidar-derived elevation products (Rowley et al., in review; Willis et al., in review).

Mapping of Quaternary-active faults and folds in Utah is continually incorporated into the *Utah Geological Hazards Portal* (https://hazards.geology.utah.gov/, Utah Geological Survey, undated). This online map and database started with the first statewide compilations by Anderson and Miller (1979) and Hecker (1993) of Quaternary faults and folds in Utah. In 2003, Hecker's comprehensive database was updated and expanded by Black et al. (2003) as Utah's contribution to the creation of the USGS *Quaternary Fault and Fold Database of the United States*. The *Utah Quaternary Fault and Fold Database* was first published online in 2016, and incorporated into the *Utah Geologic Hazards Portal* in 2020, and maintains general compatibility with the current *Quaternary Fault and Fold Database of the United States* (U.S. Geological Survey, undated [a]) by using guidelines set by Haller et al. (1993).

DATA SOURCES

Lidar Elevation Data

We used USGS QL1 and QL2 (0.5- and 1-m-pixel resolution, respectively; Heidemann, 2018) lidar elevation datasets (Utah Geospatial Reference Center, 2016, 2018, and 2020) to create derivative products, including digital elevation models (DEMs) that were useful for identifying and refining surficial fault traces. Additionally, the USGS's 3DEP Raster Image Service (https://www.usgs.gov/the-national-map-data-delivery/applications-visualization-services) was used in ESRI ArcPro software for lidar derivative products. These derivative products include DEM-derived slopeshade images, various hillshade images with different light directions and altitudes, and contour lines. GlobalMapper (v.18 and v.23) and ESRI ArcPro software was used to generate these images, as well as to generate topographic profiles perpendicular to scarps to investigate fault-scarp morphologies.

Aerial Photography

Historical aerial photography stereo pairs from the UGS *Aerial Imagery Collection* (https://geodata.geology.utah.gov/imagery/) were used throughout the investigation. These photographs were most useful for mapping in urban areas, where surface fault traces have been obscured by modern ground disturbance. Aerial photograph sets from 1958 (Farm Service Agency, 1953–1961) and 1975 (U.S. Bureau of Land Management, 1975) were used for mapping around some of the urban areas within the study area.

Previous Geologic Mapping

Of the previously published geologic maps in the area (listed above), we used those that are 1:24,000 scale as well as the most recent 1:100,000 scale. The newer 1:100,000-scale geologic maps (Hintze and Davis, 2002; Rowley et al., 2005; Witkind et al., 2007; Hintze et al., 2008; Rowley et al., in review; Willis et al., in review) were particularly useful throughout the project area. Geologic maps contribute important surficial unit age information, which is used for determining fault structure age categories (described below) given to mapped fault scarps in this study. Many of these maps (both UGS and USGS publications) are available through the UGS's *Interactive Geologic Map Portal* (https://geomap.geology.utah.gov/) for digital viewing and downloads as GeoTiff or GIS files.

METHODS

Fault Mapping

Fault traces were mapped according to UGS best practices and the experience of the authors. Each mapper used complementary techniques to best identify fault scarps indicative of previous surface-fault rupture or deformation. The lidar DEMs and derivative products such as slope-angle (or slopeshade) maps, slope-aspect maps, and various light direction and altitude hillshade images proved to be the most useful tools when mapping the faults in the central Utah region. Tightly spaced topographic contour lines generated from DEMs were particularly useful when differentiating between fault scarps and other geomorphic features.

In areas of urban development, pre-development stereo-paired aerial images were used to identify and map fault traces as well as investigate other lineaments. These photos were particularly useful in identifying fault traces that have been obscured by development.

Fault Attributes

We attributed mapped faults following the conventions used in the *Utah Geologic Hazards Portal* and previous UGS fault mapping publications (McDonald et al., 2020, Hiscock et al., 2021, Hiscock et al., 2024; Knudsen et al., 2021). Fault attributes include fault/fault zone name, fault segment name (if applicable), structure/fault number, mapped scale, fault dip direction, fault mapping constraint, slip sense, slip rate category, structure class, and structure age category. These attributes generally follow those established by Haller et al. (1993) for the USGS *Quaternary Fault and Fold Database of the United States*.

Across Utah, basic attributes of faults (e.g., dip direction, slip sense) are mainly determined from surficial mapping and lidar elevation data, and in some cases, refined by field reconnaissance or natural or man-made exposure. The structure age category and slip rate category are more difficult to determine as most Utah Quaternary faults lack paleoseismic data. Updates of these attributes in the *Utah Geologic Hazards Portal* are completed using the most recent geologic information available.

Structure age categories in the *Utah Geologic Hazards Portal* and the USGS *Quaternary Fault and Fold Database of the United States* reflect the best available timing information for the most recent surface-rupturing earthquake on a fault trace. The last suspected paleo-event (Haller et al., 1993; Crone and Wheeler, 2000) is inferred from fault surface expression and geomorphic relationships, previous Quaternary geologic mapping, reconnaissance of fault scarps, and paleoseismic data (where available). The UGS uses the age categories framework originally established by Haller et al. (1993) and adopted by Lund et al. (2020) with the addition or revision of age categories based on best practices within the paleoseismic community. The age categories currently used include:

- Latest Pleistocene to Holocene – a fault whose movement in the past 15,000 years before present has been large enough to break the ground surface.
- Late Quaternary – a fault whose movement in the past 130,000 years before present has been large enough to break the ground surface.
- Middle Quaternary – a fault whose movement in the past 750,000 years before present has been large enough to break the ground surface.
- Quaternary – a fault whose movement in the past 2.6 million years before present has been large enough to break the ground surface.

We categorized Quaternary faults in the central Utah region as "well constrained," "moderately constrained," or "buried or inferred" fault traces. We consider a fault well constrained if its trace is clearly detectable by a trained geologist as a physical feature on the ground surface (Bryant and Hart, 2007). We consider a fault moderately constrained when the fault is less clearly detectable by a trained geologist on the ground surface, i.e., the fault scarp has been modified by erosional processes and is less apparent on high-resolution elevation data versus a well constrained fault. We mapped a fault as buried/inferred when the trace of the fault is not evident at the ground surface, or on high-resolution elevation data, i.e., it is likely buried by younger alluvial fans, other unconsolidated deposits, or anthropogenic modification.

The reasons for the lack of clear surface evidence for buried/inferred faults are varied, but are chiefly related to one or more of the following causes: (1) long earthquake recurrence intervals and a long elapsed time since the most recent surface-faulting earthquake allowing subsequent erosion and deposition to obscure surface evidence for the faults; (2) rapid deposition that quickly obscures faults, even those with comparatively short recurrence intervals; (3) faulting that generates relatively small scarps (<3 feet [<1 m]) that are quickly obscured, and (4) faulting that occurs at or above the bedrock/alluvium contact in relatively steep terrain and is difficult to identify. Although not evident at the surface, these faults still may represent a significant surface-fault-rupture hazard and should be evaluated prior to development in areas where they may rupture to the ground surface. Additionally, lineaments that we were unable to conclusively determine as fault-related were mapped as "lineaments." These lineaments are included in the geodatabase with this report, but not in the *Utah Geologic Hazards Portal*.

Special-Study Zone Delineation

We delineated recommended surface-fault-rupture special-study zones for faults mapped in the central Utah region. These zones are delineated along active faults in accordance with Utah State Code 79-3-202(f) and define areas where additional investigation is recommended to evaluate the risk from surface faulting prior to residential, business, and infrastructure development (Lund et al., 2020). Together with the fault traces, these special-study zones are critical to the creation and implementation of municipal and county geologic-hazard ordinances associated with hazardous faults and understanding surface-rupturing hazard and associated risk.

Special-study area dimensions are based on the *Guidelines for Evaluating Surface-Fault-Rupture Hazards in Utah* (Lund et al., 2020). For well constrained faults, the special-study zones extend 500 feet (152 m) on the downthrown side and 250 feet (76 m) on the upthrown side of each fault. For moderately constrained and buried or inferred faults, the special-study zones extend 1000 feet (305 m) on each side of the suspected trace of the fault.

Several criteria were established for distinct circumstances pertaining to fault-related special-study zones (Figure 3). For traces of buried/inferred or moderately constrained faults less than 1000 feet (305 m) long that lie between and on-trend with well constrained faults, the well constrained fault special-study-area criteria were used (Figure 3A). For buried/inferred or moderately constrained faults greater than 1000 feet (305 m) long, the special-study area includes 1000 feet (305 m) on both sides of the fault. For inferred faults at the end of a mapped fault trace that are longer than 1000 feet (305 m), we used an inferred fault special-study area (Figure 3B). In areas where a buffer "window" exists (a space between the special-study zones of two sub-parallel fault traces), we include the window in the special-study zone if its width is less than the greater of the two surrounding special-study zones (Figure 3C). For a complete description of surface-fault-rupture special-study zones see Lund et al. (2020).

Identification of Potential Paleoseismic Investigation Sites

We analyzed each mapped fault for potential paleoseismic investigation sites as part of our fault-trace mapping (Table 1). Fifty-seven sites were identified based on: (1) the presence of a normal, preferably single fault scarp, (2) scarp heights logistically reasonable for excavating a paleoseismic trench (roughly 2–30 feet [0.5–10 m]), (3) visible displacement of young deposits (Late Pleistocene to Holocene), and (4) surfaces and scarps mostly undisturbed by residential, business, and infrastructure development activities. Sites that could fill in data gaps between previous paleoseismic investigations and sites within areas of ongoing development were considered even if they did not meet all four criteria. Due to the rural and undeveloped nature of central Utah, many sites were identified that are not discussed in detail in this report.

The 57 potential paleoseismic sites (Table 1) should not be considered a complete list of all sites identified in this study, as additional sites may exist. This dataset was designed to assist the UGS, USGS, and other paleoseismic investigators in determining future sites for paleoseismic investigation.

Because paleoseismic investigation opportunities are limited by funding availability and time constraints, the UGS works to maintain a relationship with local geologic and engineering consultants who conduct trenching investigations for clients along faults in Utah. The UGS is often invited to visit consultant trenches for a few hours to observe and document faulting, and in some cases collect age dating samples for earthquake timing information. Although not as useful as a full paleoseismic research investigation, these site visits still provide useful information in areas where we will most likely never be able to conduct a full research-level investigation.

FAULT MAPPING AND POTENTIAL PALEOSEISMIC SITES

The main features mapped in this study are topographic escarpments (scarps) interpreted to be formed by past surface-rupturing earthquakes in central Utah. The following sections discuss the character and geomorphology of each mapped fault (fault names are from the *Utah Geologic Hazards Portal*). Faults are presented in geographic order, from north to south (Figures 4, 5, and 6). Descriptions include

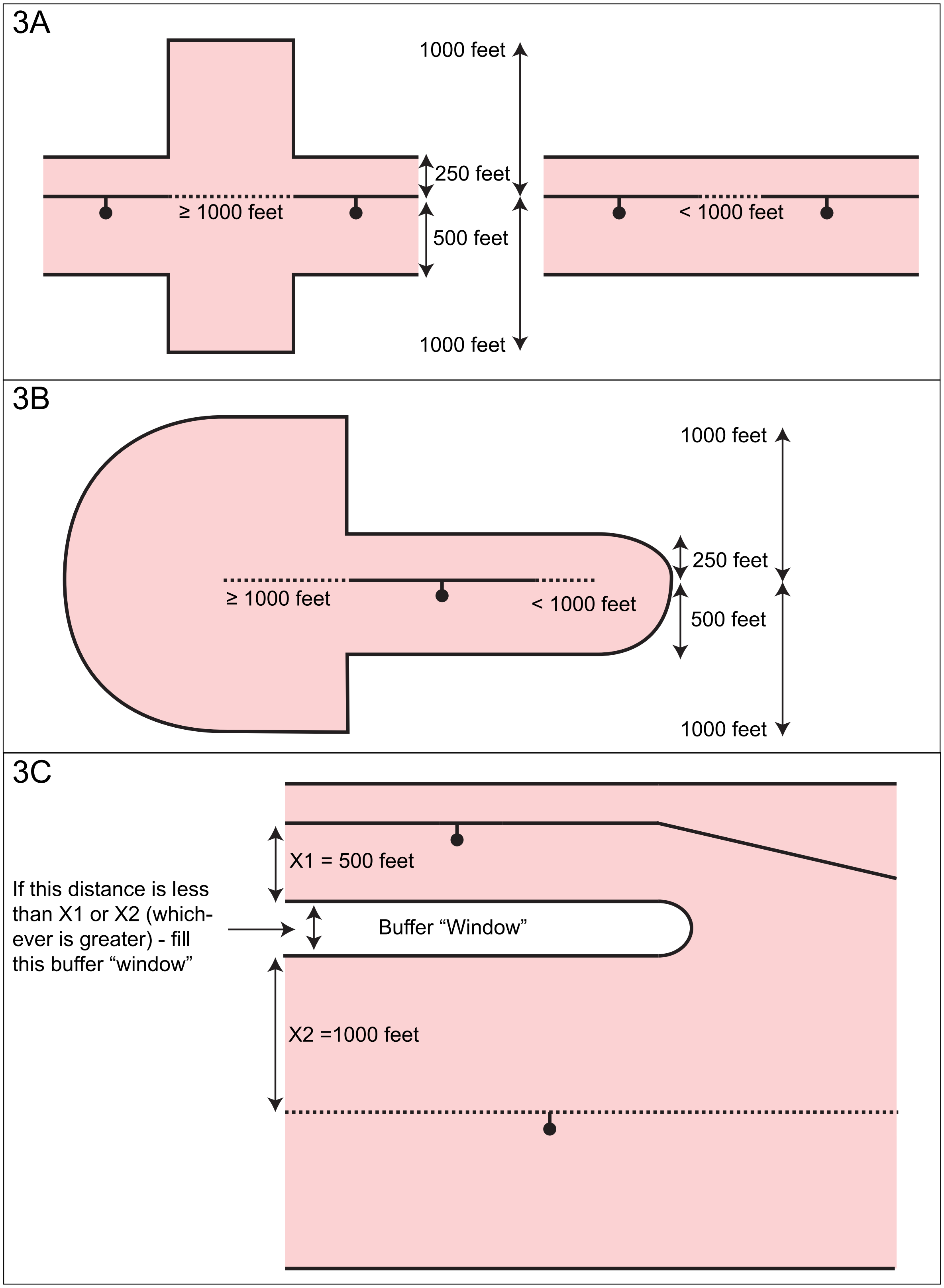

Figure 3. *Examples of special circumstances used when creating surface-fault-rupture special-study zones relative to mapped fault traces (after Lund et al., 2020).*

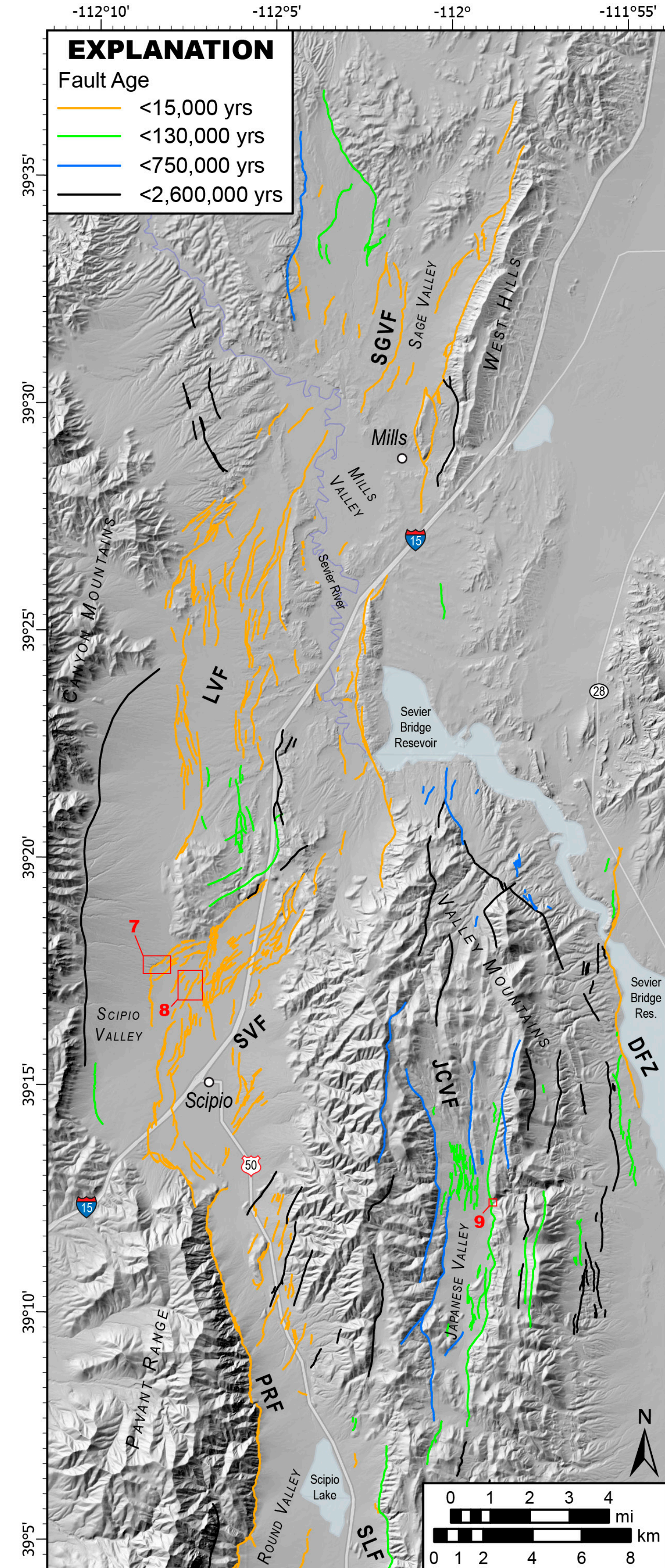

Figure 4. *Fault zones mapped as part of the northern part of this study (SGVF = Sage Valley faults, LVF = Little Valley faults, SVF = Scipio Valley faults, DFZ = Dover fault zone, JCVF = Japanese Cal Valley faults, PRF = Pavant Range fault, SLF = Scipio Lake faults; all fault names from the* Utah Geologic Hazards Portal *[undated]). Red boxes show locations of other figures. Shaded relief base map from USGS 3DEP Program.*

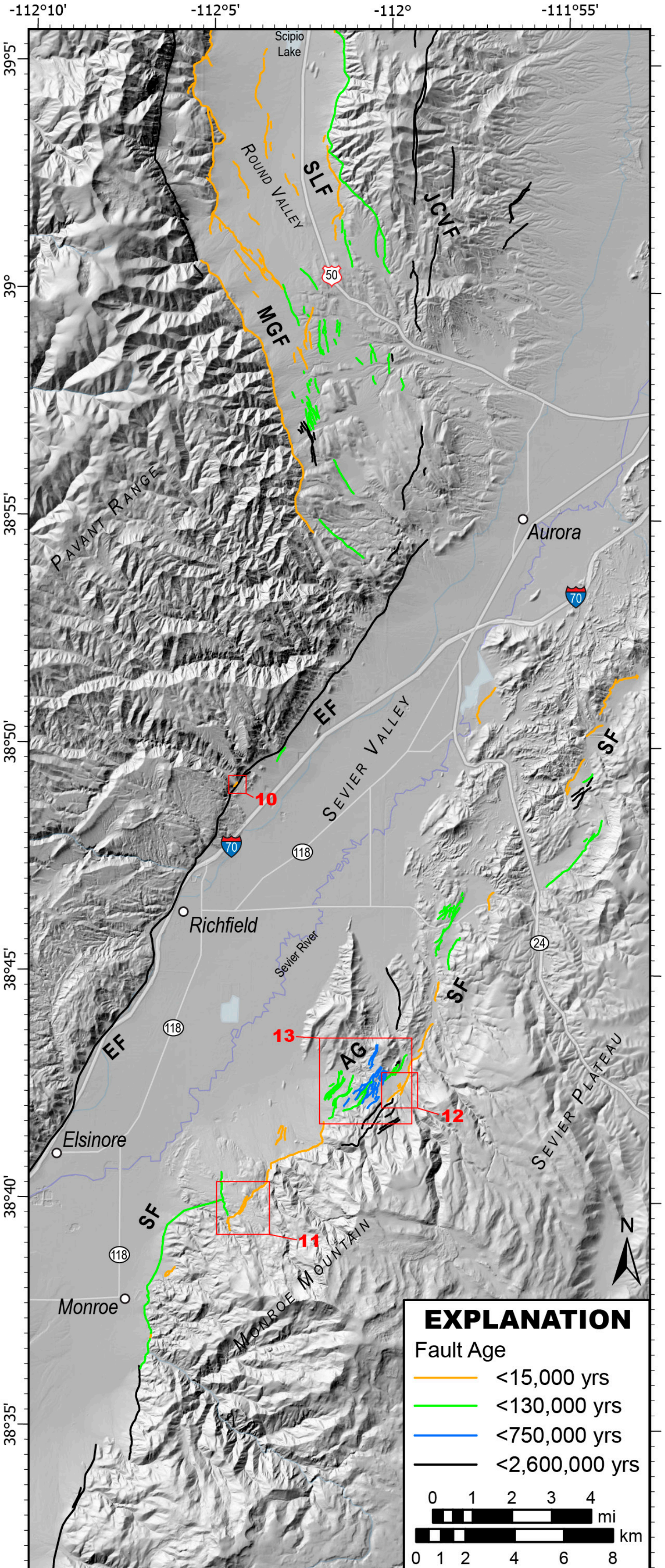

Figure 5. *Fault zones mapped as part of the central part of this study (SLF = Scipio Lake faults, MGF = Maple Grove faults, JCVF = Japanese Cal Valley faults, EF = Elsinore fault, SF = Sevier fault, AG = Annabella graben; all fault names from the* Utah Geologic Hazards Portal *[undated]). Red boxes show locations of other figures. Shaded relief base map from USGS 3DEP Program.*

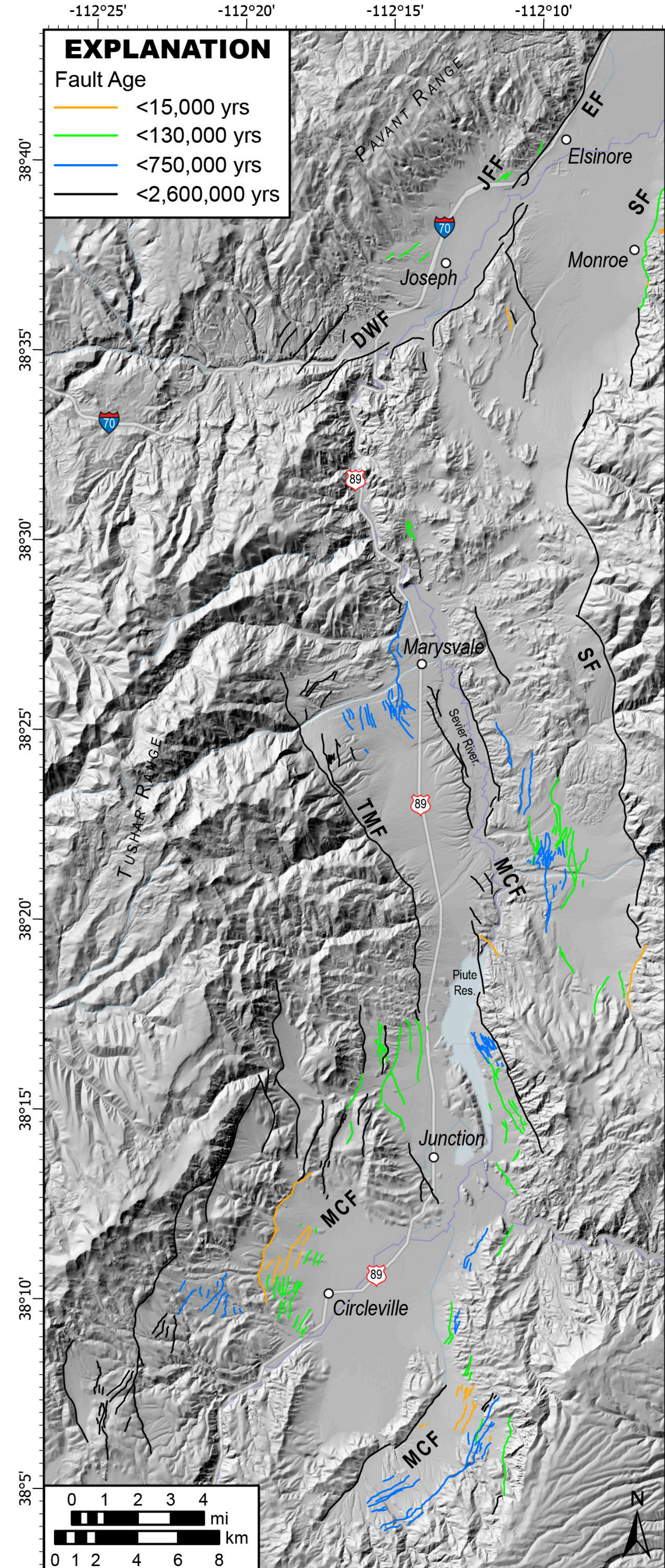

Figure 6. Fault zones mapped in the southern part of this study (EF = Elsinore fault, JFF = Joseph Flats faults, SF = Sevier fault, DWF = Dry Wash fault and folds, TMF = Tushar Mountains (east side) fault, MCF = Marysvale–Circleville area faults; all fault names from the Utah Geologic Hazards Portal *[undated]). Shaded relief base map from USGS 3DEP Program.*

the character of each fault as well as what specific data and previous studies and maps (if available) that were used to interpret the location, extent, and age category of faulting. Additionally, the location and details about potential paleoseismic trenching sites (Table 1) are included.

Sage Valley Fault

Named and mapped by Clark (2003), the Sage Valley fault has formed a prominent, linear bedrock escarpment along the base of the West Hills (Figure 4). The fault generally places Tertiary bedrock against Late Pleistocene to Holocene alluvial-fan deposits of Sage Valley (unit Qaf1 of Clark [2003]). About 2.5 miles (~4 km) north-northeast of Mills, the Sage Valley fault has formed a 3-foot-high (1 m) scarp near the apex of an alluvial fan that is consistent with a latest Pleistocene to Holocene (<15 ka) rupture. Trenching along this scarp is the best opportunity to develop detailed paleoseismic data for the Sage Valley fault.

In addition to the main west-dipping Sage Valley fault that bounds the eastern side of Sage Valley, we mapped several east- and west-dipping faults that have formed scarps on both bedrock and unconsolidated units throughout Sage Valley. We collectively refer to all mapped faults in the valley as the Sage Valley faults (SGVF). Based on scarp morphology and the estimated ages of geologic units cut, most additional faults in Sage Valley are classified as latest Pleistocene to Holocene (<15 ka) or late Quaternary in age (<130 ka). Exceptions are the westernmost faults that are largely exposed in bedrock and have only a few poorly preserved scarps formed on older (Middle to Late Pleistocene) alluvium; these were assigned to the middle Quaternary age category (<750 ka).

Little Valley Faults

The Little Valley faults (LVF) form a wide zone of faulting north of Scipio Valley, bounded on the north by the Sevier River, on the west by the Canyon Mountains, and on the east by Sevier Bridge Reservoir (Figure 4). Based on scarp morphology and cross-cutting relations with surficial units, the apparent ages of scarps on the LVF range from early Quaternary to Holocene. We mapped poorly preserved scarps formed on older alluvial-fan deposits (Pliocene to Middle Pleistocene QTaf of Oviatt and Hintze [2005]), and on Cretaceous/Tertiary bedrock as Quaternary active (<2.6 Ma). The youngest LVF scarps are formed on Holocene Sevier River floodplain deposits (unit Qalf of Oviatt and Hinze [2005]) west of Mills. Gerhart Consultants (2003) trenched one of the faults, known as the Badeau Ridge fault, that has formed a prominent bedrock escarpment north of Sevier Bridge dam. Based on estimated ages of displaced unconsolidated units revealed in their trenches, they found evidence for at least two Holocene surface-rupturing events.

We mapped several discontinuous, narrow (<30 feet [<10 m] wide), and subtle (<3 feet [<1 m] deep) grabens formed on alluvium adjacent to the Sevier River. A cluster of such grabens are mapped north of U.S. Interstate 15 on the west side of the Sevier River in Mills Valley (Figure 4). Additional clusters of grabens are on both sides of the Sevier River between U.S. Interstate 15 and Sevier Bridge dam. The proximity and general alignment of the grabens to the Sevier River may link the formation of these scarps to the dissolution of underlying water-soluble rock. Since the origins of the grabens are questionable, we consider them to be Class B structures.

Dover Fault Zone

The Dover fault zone (DFZ) runs along the eastern range front of the Valley Mountains (Figure 4), forming a narrow zone on-trend with the south end of the Wasatch fault zone; specifically, the south end of the Levan segment and Levan-Fayette segment boundary scarps and lineaments (Hylland and Machette, 2008; Hiscock and Hylland, 2015). Fault scarps on the DFZ cut primarily pediment-mantle alluvium (Qap) which is estimated to be Late Pliocene to Early Pleistocene in age (Peterson, 1997; Willis, 1991). Hylland and Machette (2008) first mapped these older fault scarps before the advantage of lidar data. We have identified a new fault scarp cutting young Holocene deposits, running roughly parallel and just above the highstand shorelines of the Sevier Bridge Reservoir (Figure 4). Several fault scarps suitable for paleoseismic trenching exist along this young scarp and would present a good opportunity to collect additional paleoseismic data on the DFZ. These new data could be compared with data on the southern Wasatch fault zone, specifically the Levan and Fayette segments (McDonald et al., 2019) to determine any paleoseismic connection between these on-trend fault systems.

Running along the east side of the Valley Mountains is the Valley Mountains monocline. This monocline was previously included in older versions of the *Utah Quaternary Fault and Fold Database* and the current version of the *Utah Geologic Hazards Portal* as a Class B structure. We exclude this structure from our mapping and the *Utah Geologic Hazards Portal* as it includes no surficial expression or direct evidence of any Quaternary-age activity. It is possible that the normal faulting associated with the DFZ may be driven by the Valley Mountains monocline (Peterson, 1997). Witkind (1994) theorized the monocline may have been formed by collapse features possibly related to the dissolution of salt-bearing Jurassic Arapien Shale at depth, driven by groundwater flow to the Sevier River from the Valley Mountains. However, the lack of salt-bearing rocks in an oil well drilled on the Redmond quadrangle could rule out the role of salt dissolution in the creation of the Valley Mountains monocline (Standlee, 1982; Peterson, 1997). We did not observe any evidence that any faults associated with the DFZ are non-seismogenic, therefore, we leave the DFZ as a Class A structure.

Scipio Valley Faults

The Scipio Valley faults (Figure 4) have produced a broad and locally dense zone of scarps throughout the floor of Scipio Valley. Based on apparent differences in the ages of most recent rupture, Bucknam and Anderson (1979) mapped two separate fault zones in Scipio Valley that include the Scipio Valley faults consisting of a pair of right-stepping, down-to-the-southeast faults that form the boundary between northwestern Scipio Valley and the Low Hills, and the Scipio fault zone, a pair of faults that form a prominent graben west of Scipio. Black et al. (2003) followed this convention and added several additional faults mapped by Oviatt (1992) to the Scipio fault zone that expanded the fault zone well beyond the original graben. Our lidar-based mapping greatly increases the distribution and density of faulting in Scipio Valley and reveals a complex network of faulting that is difficult to separate based on the estimated ages of most recent ruptures. To avoid confusion, we abandon the name "Scipio fault zone" and group all faults in the valley into a single group of faults called the Scipio Valley faults (SVF).

SVF scarps are formed on Late Pleistocene to Holocene alluvium (units Qaf1 and Qal1 of Hintze and Davis [2002]) and are generally mapped as latest Pleistocene to Holocene active (<15 ka). An exception is an eroded and partially buried north-trending scarp formed on Late Pleistocene alluvial-fan deposits along the base of the Canyon Mountains that we map as late Quaternary in age (<130 ka). Superimposed on a 65-foot-high (20 m) composite scarp along the northwest margin of the valley (Bucknam and Anderson's [1979] Scipio Valley fault) is a youthful, well-preserved 10-foot-high (3 m) scarp (Figure 7). The younger scarp appears to be similar in age to the Fish Springs fault scarp (Bucknam and Anderson, 1979; Black et al., 2003) thought to be 2 to 3 ka (Hanks et al., 1984; Bucknam et al., 1989; Black et al., 2003). Many newly mapped SVF scarps are less than 3 to 6 feet (<1–2 m) high and are likely the result of a single surface-faulting earthquake.

Zones of elongate sinkholes and depressions formed on unconsolidated alluvium on-trend with the SVF have long been recognized in Scipio Valley (e.g., Griswold, 1948; Bjorklund and Robinson, 1968; Oviatt, 1992). The sinkholes were likely formed by piping of fine-grained sediment into fault and fracture zones in the underlying bedrock (Griswold, 1948; Bjorklund and Robinson, 1968). Our mapping confirms a strong correlation between the elongate sinkholes and faults (Figure 8). While many elongate sinkholes are formed directly along fault scarps, others are not associated with scarps and show no vertical displacement across the sinkholes. Although we suspect that most or all elongate sinkholes are related to underlying faults and fractures, we did not map elongate sinkholes as faults unless vertical displacement across the sinkhole was detected. In addition to elongate sinkholes, we observed subtle (<3 feet [<1 m] high and <30 feet [<10 m] wide) elongate mounds as much as 2000 feet (600 m) long that share

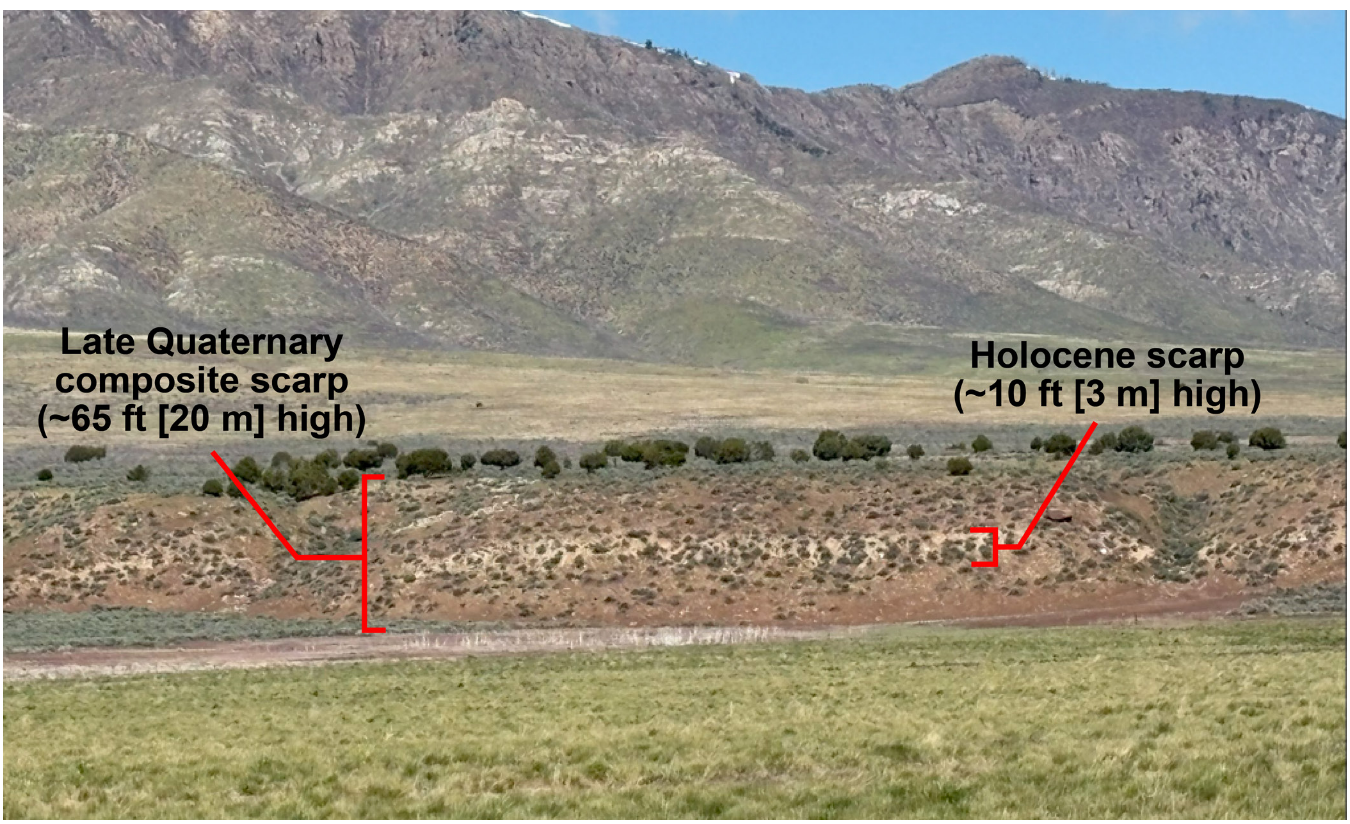

Figure 7. *Composite Scipio valley scarp about 3 miles (~5 km) north-northwest of Scipio. View is westward toward the Canyon Mountains. Photo taken May 1, 2025.*

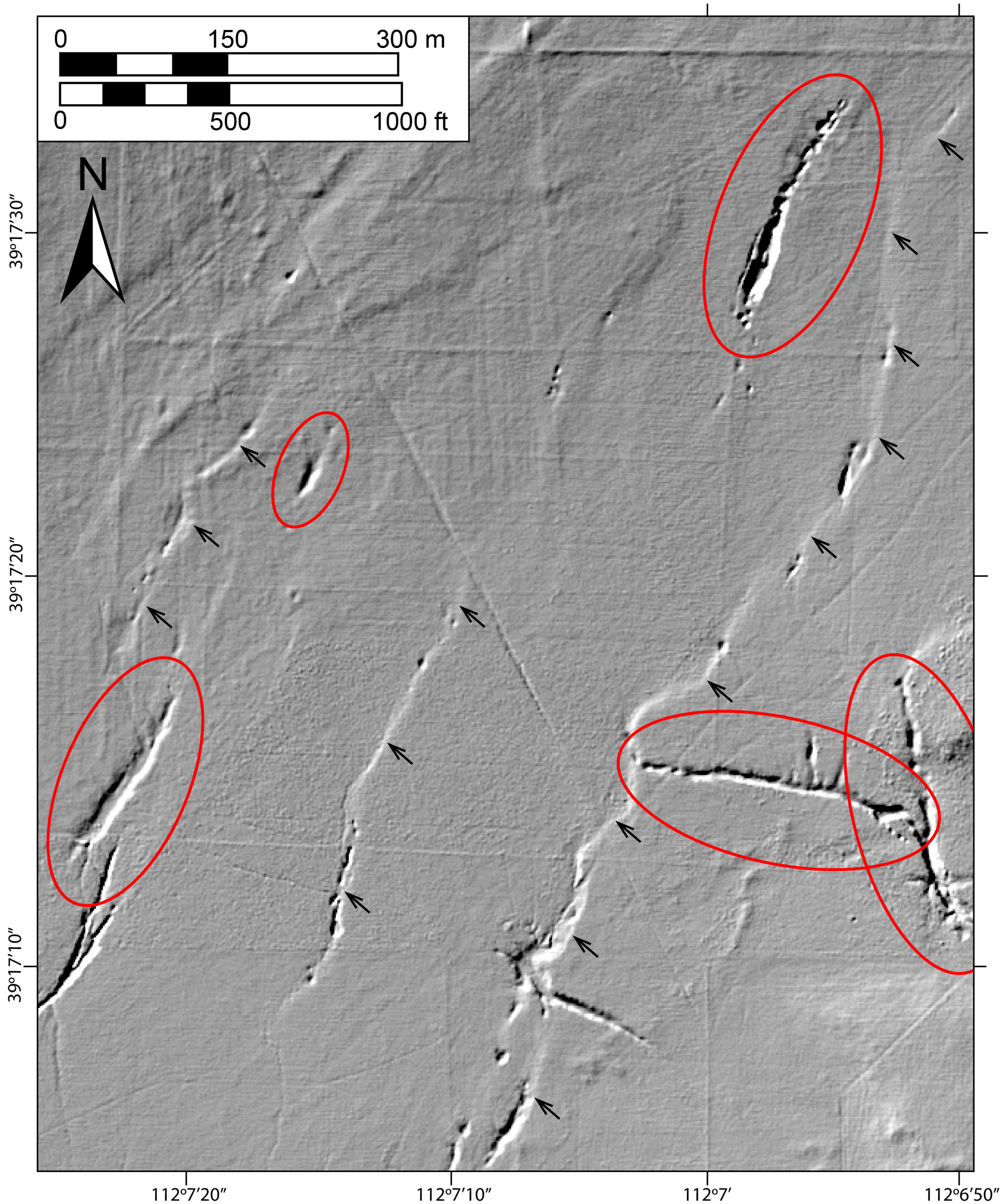

Figure 8. *Lidar hillshade image of west-central Scipio Valley showing the close relationship of elongate sinkholes with fault scarps. Small arrows indicate prominent fault scarps. Red ellipses highlight larger elongate sinkholes with no vertical displacement across them that were not mapped as faults in this study. Basemap from USGS 3DEP program.*

a similar trend to adjacent scarps and elongate sinkholes. The origin of the mounds are unknown, but they also may be associated with underlying faults and fracture zones. We suspect the elongate mounds are linear zones of sediment that are cemented to a greater degree than surrounding sediment, making them more resistant to erosion, and thus resulting in positive relief. The increased cementation may have precipitated out of mineral-laden surface water percolating through the surficial sediments into underlying faults/fractures. The water would have moved at a slow enough rate as to not induce piping and sinkhole formation at the surface. Regardless of their origin, no elongate mounds were mapped as faults.

Japanese and Cal Valley Faults

Japanese Valley is a north-trending, 1-mile-wide (1.6 km), fault-bounded graben that extends for 10 miles (16 km) along the axis of the Valley Mountains. Smaller half-grabens west of Japanese Valley, including Cal Valley, are controlled by faults dipping east toward Japanese Valley. Smaller grabens east of Japanese Valley have master faults that dip west, also toward Japanese Valley. Witkind et al. (2007) argued that this faulting pattern implies that the Valley Mountain grabens are collapse features possibly related to the dissolution of salt-bearing Jurassic Arapien Shale at depth. Willis (1991) attributed faulting and graben formation in the Valley Mountains to Basin and Range extension. Resolving the origin of faulting in the Valley Mountains is beyond the scope of this study, but we did not observe any evidence that counters the idea of the faults being seismogenic and we consider these faults Class A structures.

Graben-bounding faults in the Valley Mountains generally place late Quaternary unconsolidated valley-fill deposits against Tertiary bedrock. These faults are commonly concealed beneath a veneer of colluvium and slope wash. A dense zone of discontinuous, but well-preserved fault scarps formed on moderately dissected Late Pleistocene alluvial fans on the floor of northern Japanese Valley appears to be the locus of the most recent faulting in the Valley Mountains. A natural stream cut at the head of Hayes Canyon exposes the west-dipping fault bounding the eastern margin of Japanese Valley (Figure 9). The cut reveals Late Pleistocene to Holocene(?) alluvium vertically displaced at least 3 feet (1 m) down to the west by faults that extend to within about 3 feet (1 m) of the ground surface. Many of the larger graben-bounding faults in the Valley Mountains are buried by several feet of unbroken colluvium/alluvium, or are expressed as fault-line scarps in bedrock, indicating an older age. These faults are thus assigned to the middle Quaternary (<750 ka) or Quaternary (<2.6 Ma) age categories.

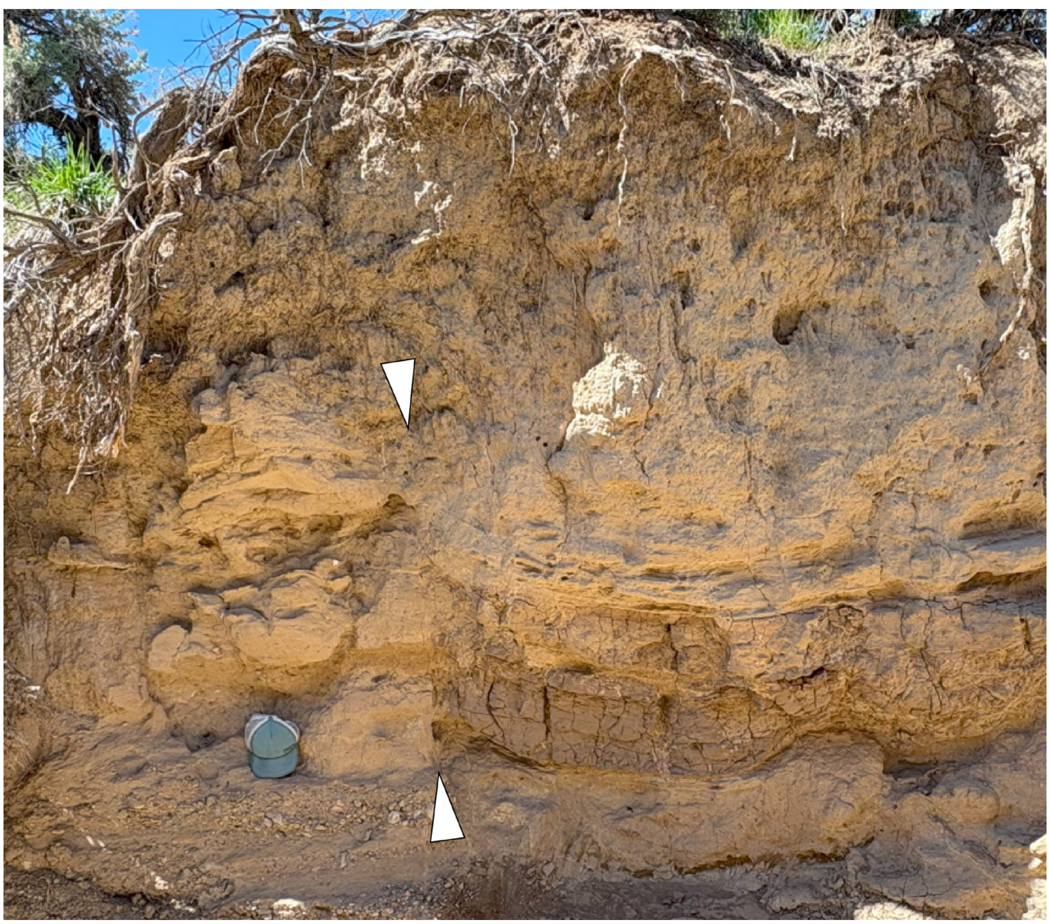

Figure 9. *Stream cut exposing faulted alluvium along the eastern margin of Japanese Valley. No scarp was detected at the surface. Vertical distance from hat to the land surface is about 2 meters. View is to the south. Photo taken May 2, 2025.*

Pavant Range Fault

The Pavant Range fault zone (PRF) runs approximately 15.5 miles (25 km) along the eastern rangefront of the Pavant Range, following a north-south trend (Figure 4). The zone is bounded by the Scipio Valley faults to the north and the Maple Grove faults to the south. The zone is characterized by complex east-dipping faults with multiple graben-bounded west-dipping faults. The faults primarily cut the Cretaceous Canyon Range Conglomerate (Kc) and younger alluvial-fan deposits thought to be Holocene in age (Oviatt, 1992).

New mapping shows complexities in the fault traces along the rangefront with well-preserved scarps measuring ~18 feet (5.5 m) high. These well-preserved scarps are often located within older alluvial-fan deposits at the mouths of canyons (Bucknam and Anderson, 1979). The faulting is characterized by scarps formed on alluvial-fan deposits towards the northern section of the fault zone and by oversteepened range fronts and linear valleys/drainages towards the southern section of the fault zone. Several scarps along the PRF in similar geomorphic settings are suitable for paleoseismic trenching studies (Table 1). Within Round Valley (Figure 4), scarps are apparent in unconsolidated alluvial-fan deposits. We changed the extent of this zone to include the southern part into Round Valley (Figure 4; previously mapped as a part of the Maple Grove faults) as the fault geometry is continuous and we wanted to accurately represent the entirety of the fault.

Maple Grove Faults

The Maple Grove faults (MGF) are situated along the eastern flank of Round Valley, which separates the Pavant Range and Valley Mountains (Figures 4 and 5). The majority of the faults dip east, with several smaller graben-bounding west-dipping scarps. Faults previously mapped as the Red Canyon fault scarps have been consolidated into the MGF, adding approximately 5 miles (8 km) to the southern end of the fault zone.

The geomorphic expression of MGF scarps is steeper than PRF scarps, likely due to variable coarseness of the alluvium (Bucknam and Anderson, 1979). Many of the range front faults place late to middle Quaternary deposits against Tertiary bedrock and are placed in the Holocene (<15 ka) age category. These faults also display the largest offset, indicating multiple events (Oviatt, 1992). There are several places where the faults extend into Tertiary bedrock, and these traces are placed in the Quaternary (<2.6 Ma) age category. The southernmost fault trace is mapped mostly in Tertiary-age deposits with some offset apparent in Late Pleistocene alluvial fans, is assigned to the <130 ka age category. This trace was not previously mapped by Oviatt (1992).

Scipio Lake Faults

The Scipio Lake faults (SLF) are located within Round Valley and along the western rangefront of the Valley Mountains (Figures 4 and 5). New mapping shows many discontinuous faults located within the valley that are categorized as Pleistocene to Holocene active (<15 ka). There appears to be no general trend to the dip direction of the valley faults. Within the valley, there are small but noticeable elongate sinkholes along some of the fault traces, similar to those observed in Scipio Valley and described above (Griswold, 1948; Bjorklund and Robinson, 1968; Oviatt, 1992). On the eastern side of the valley, along the Valley Mountains rangefront (Figures 4 and 5), deflected and beheaded streams are apparent along the surficial expression of the fault. The southern end of the SLF includes a set of complex, discontinuous faults within an eroding area of Tertiary bedrock within the valley. Depending on whether the faults are mapped into the younger alluvial-fan deposits on the northern and southern end of this area or mapped entirely within the bedrock, they are assigned either a middle Quaternary (<750 ka) or Quaternary (<2.6 Ma) age category, respectively.

Elsinore Fault (Fold)

The Elsinore fault (EF) trends northeast along the western margin of Sevier Valley, forming the eastern structural boundary of the Pavant Range (Figures 5 and 6) (Willis, 1994). Previous fault mapping included one short, discontinuous scarp near the southern end of the fault zone near its junction with the Dry Wash fault, with the remainder of the fault mapped as a monoclinal fold (Anderson and Bucknam, 1979). Previous geological mapping shows Tertiary to Quaternary warping in alluvial-fan surfaces near the northern end of the structure, but did not identify any young fault scarps (Willis, 1988, 1994; Hintze et al., 2008).

Our new mapping mostly agrees with previous geologic mapping, except for one short, young, fault scarp mapped at the mouth of Willow Creek Canyon (Figure 10) just north of Richfield, Utah (Figure 5). We mapped this fault trace as Holocene-age, due to it cutting very young fan material (unit Qaf1 of Hintze [2008]) in the mouth of Willow Creek Canyon (Figure 10). This site is a viable paleoseismic trenching site and represents the only opportunity to gather paleoseismic data on the EF.

The majority of the EF is mapped as a buried/inferred fault trace, except for a few locations where subtle faulting is observed in Quaternary-Tertiary units. We chose to include the whole length of this fault, despite the lack of scarps preserved on Quaternary units along the fault. The southeastern margin of the Pavant Range has a very linear range front along the inferred trace of the EF, indicating some Quaternary displacement. Willis (1994) suggested the EF is monoclinal in nature south of Richfield, and a fault zone to the north, due to the strong, steep, and sharp range front north of Richfield. Our mapping mostly confirms this hypothesis.

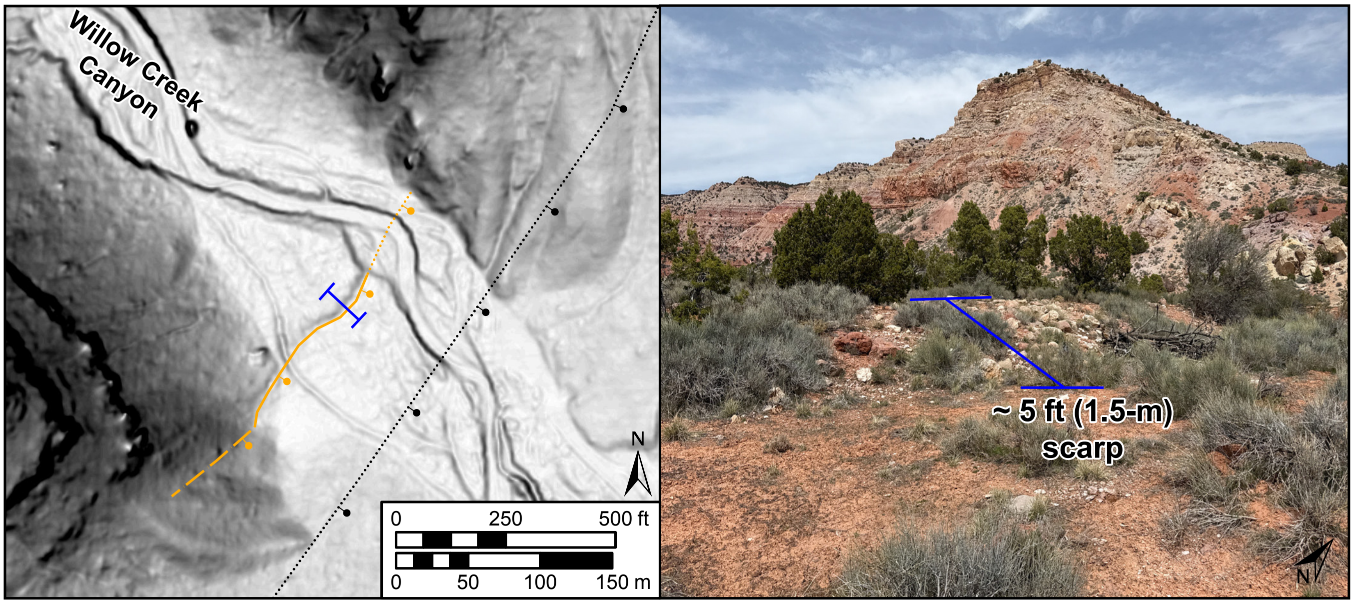

Figure 10. *Left: Lidar slopeshade image of the mouth of Willow Creek Canyon and the Elsinore fault (mapped in this study). Blue lines indicate location of fault scarp shown in photo on right. Basemap from USGS 3DEP program. Right: Photo of approximately 5-foot -high (1.5 m) fault scarp in the mouth of Willow Creek Canyon. Photo taken April 6, 2025.*

Sevier Fault

In Hecker's (1993) Quaternary faults compilation, the Sevier fault (SF) was included as part of the Sevier/Toroweap fault zone—a major, 155-mile-long (250 km) normal fault stretching from south of the Colorado River in Arizona into central Utah. Subsequently, in Black et al.'s (2003) Quaternary faults compilation, the SF was removed from the Sevier/Toroweap fault zone and changed to a separate, distinct fault. This change was justified by an approximately 30-mile (50 km) gap in surface expression between the northernmost Sevier/Toroweap fault zone and the southern end of the SF. Our new mapping has not uncovered any additional surficial fault traces in the vicinity of this gap; therefore, we chose to keep the SF as a separate structure from the Sevier/Toroweap fault zone following Black et al.'s (2003) Quaternary faults compilation. However, the SF is broadly along strike of the Sevier/Toroweap fault zone (Anderson and Barnhard, 1992) and they both represent large, normal faults along the Basin and Range–Colorado Plateau transition zone. More study is needed to determine the relationship between these two, similar, normal faults.

The SF in the southern part of our mapping area is a west-dipping buried fault along the base of the Sevier Plateau and Monroe Mountain (Figures 5 and 6). Approximately 5000 feet (1500 m) of cumulative displacement has been estimated along this part of the fault (Rowley et al., 1979a). Farther north, near Richfield, total cumulative displacement is estimated to exceed 6000 feet (1800 m) (Willis, 1994). The SF and EF form a graben containing the Sevier Valley (Figures 5 and 6).

Near the town of Monroe (Figures 5 and 6), scarps along the SF become more prominent and cut younger deposits as opposed to the mostly buried nature of the fault to the south. Just northeast of Monroe, along the western flank of Monroe Mountain, the SF cuts across a very prominent Quaternary-age landslide deposit (Qms) (Figure 11). Scarps formed on the landslide deposit are very sharp, suggesting Holocene activity. At several locations, the main scarp on landslide deposits is approximately 29.5 feet (9 m) high, suggesting evidence for multiple scarp-forming earthquakes (Figure 11). The fault bifurcates across the Qms deposit forming several small antithetic faults and narrow, subtle grabens. These scarps were mapped originally by Rowley et al. (1981b) and included on the Richfield 30′ x 60′ geologic map (Hintze et al., 2008).

Several sites suitable for paleoseismic trenching were identified at and near where the SF cuts this Qms deposit near the mouth of Thompson Canyon (Figure 11). These represent one of the best opportunities for trenching the SF in the study area due to their proximity to the rapidly growing Richfield/Sevier Valley region and the rural, undeveloped nature of the area. North of the Qms deposit, several other trench sites were identified that may also be suitable for trenching. However, the scarps at these sites are less prominent than the scarps cutting Qms.

Continuing north, the SF trends into and along the east side of the Annabella Graben (AG) zone of faults. The AG is likely associated with the SF but has its own name and fault number in the *Utah Geologic Hazards Portal*. Again, more study and paleoseismic data is needed to determine the relationship between the AG and the SF. The SF continues along the rangefront to the east of the AG. We mapped a prominent, Holocene (<15 ka) scarp along the eastern margin of Sauls Meadow Valley (Figure 12). Several sites suitable for paleoseismic trenching are located along this

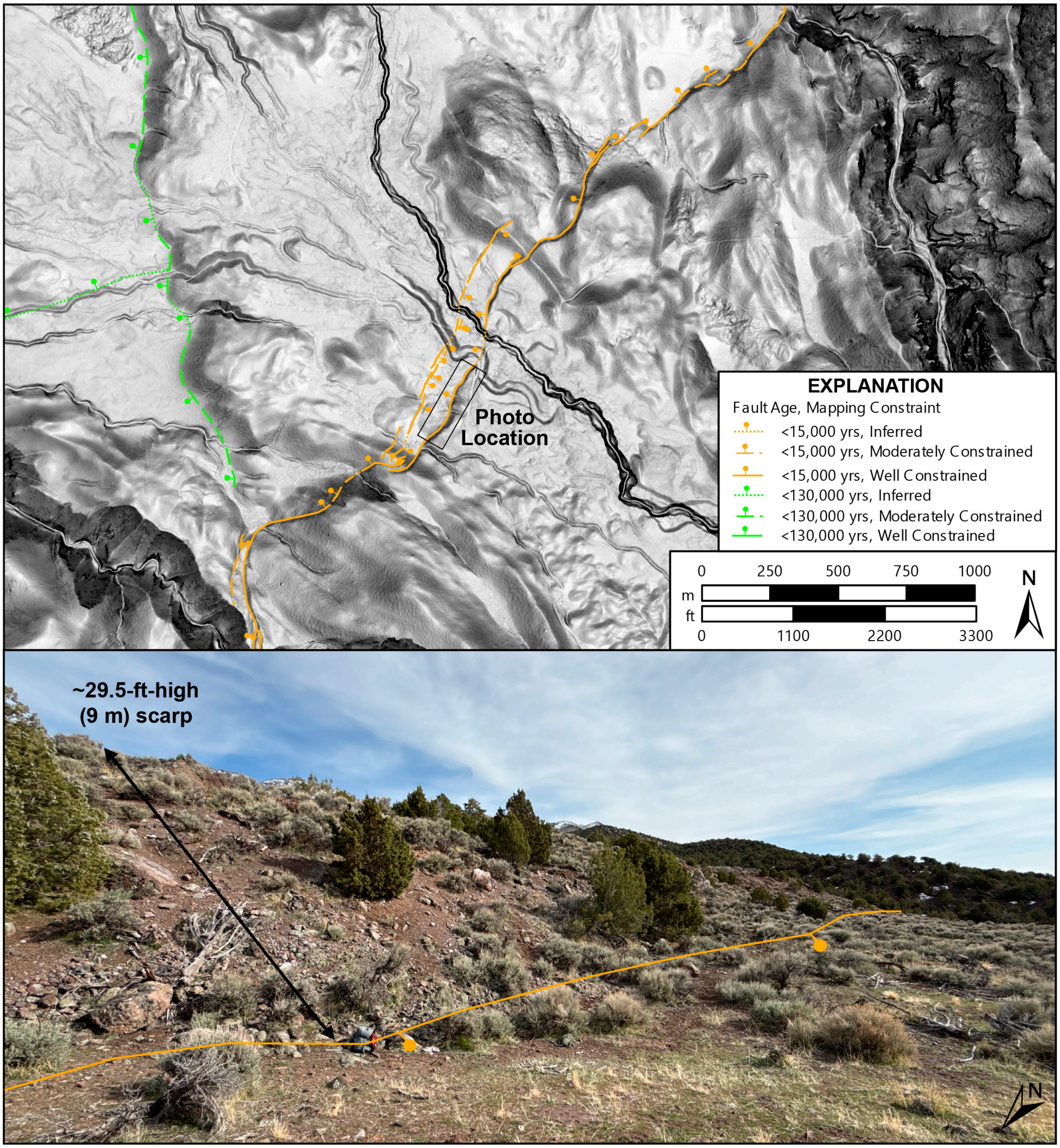

Figure 11. *Top: Lidar slopeshade image of the mouth of Thompson Canyon area, showing Qms deposit cut by young fault scarps. Fault mapping of the Sevier fault zone shown (from this study). Basemap from USGS 3DEP program. Bottom: Photo of approximately 29.5-foot-high (9 m) fault scarp (location shown in lidar image above) at the mouth of Thompson Canyon on the Sevier fault zone. Orange line shows approximate trace of fault (bar balls indicate downdropped side of fault). Photo taken April 7, 2025.*

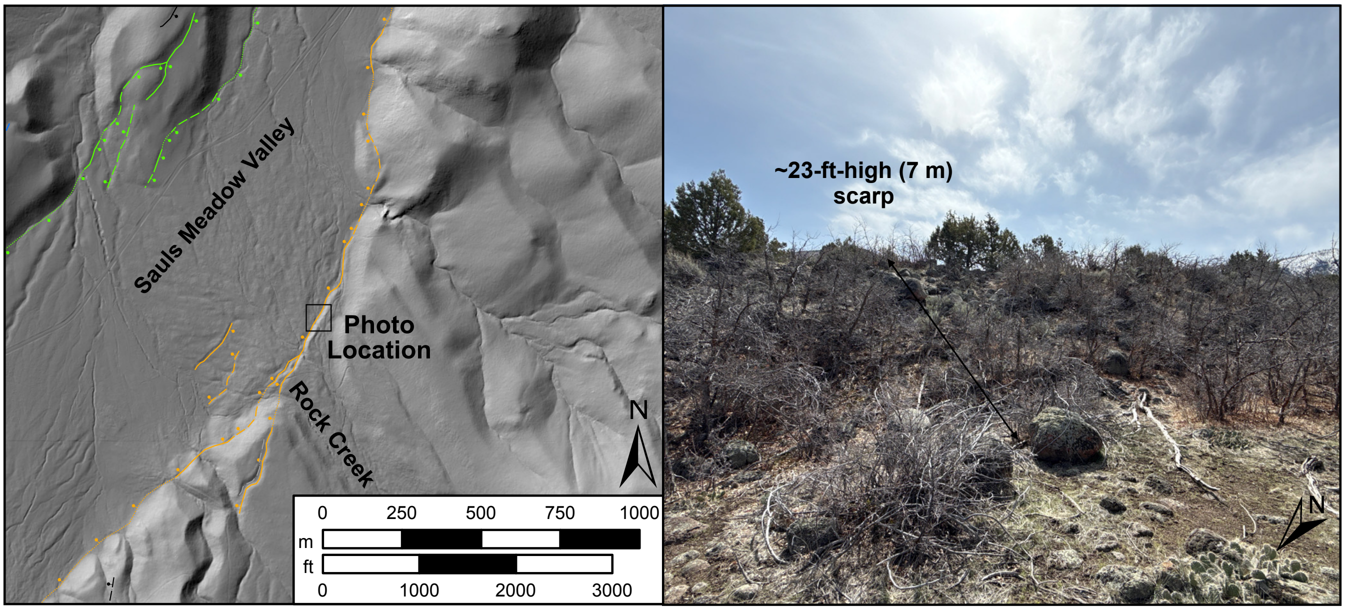

Figure 12. *Left: Lidar hillshade image of the mouth of Rock Creek Canyon, fault mapping of the Annabella Graben shown (from this study). Basemap from USGS 3DEP program. Right: Photo of approximately 23-foot-high (8 m) fault scarp in the mouth of Rock Creek Canyon. Photo taken April 5, 2025.*

continuous, young scarp. The most ideal site is at the mouth of Rock Creek where the scarp displaces young alluvial deposits, making it an ideal area for future paleoseismic study (Figure 12).

Annabella Graben Faults

The AG is a zone of Late Pleistocene to early Holocene faulting approximately 1 mile (1.6 km) west of the main trace of the Sevier fault zone (Figures 5 and 13). The AG consists of a broad zone of west- and east-facing fault scarps, extending continuously for nearly 8 miles (13 km), with individual fault segments extending generally less than 3 miles (5 km) (Figure 13). The AG is potentially related to the Sevier-Sanpete monocline due to its location at the very southern end of the monocline (Anderson and Bucknam, 1979). The scarps that make up the graben are mostly formed on alluvial fans and stream terrace gravels near the southern end, and Tertiary Sevier Formation and volcanic rocks to the north (Anderson and Bucknam, 1979). Scarps in the center of the graben reach as high as approximately 90 feet (30 m) in several locations, suggesting multiple, large surface-rupturing earthquakes have occurred in this area. Our new mapping greatly expands and adds to the detail of the AG (Figure 13).

Joseph Flats Area Faults and Syncline

The Joseph Flats area faults and syncline (JFF) encompass several small, discontinuous fault scarps north of the town of Joseph. Anderson and Barhard (1992) describe this fault zone as a structural transitional zone between the EF and Dry Wash fault and syncline (DWF). We identified several previously unmapped short, en-echelon, discontinuous fault scarps on Late Pleistocene fans (Figure 6). No potential paleoseismic sites were identified on the JFF.

Dry Wash Fault and Syncline

The DWF consists of a complex zone of poorly understood faulting and associated folding spanning the northern end of the Tushar Range and southern end of the Pavant Range. The southwestern part of the DWF shows evidence for significant left-lateral strike-slip displacement (Anderson and Barnhard, 1992). The area north of the junction of U.S. Highway 89 and U.S. Interstate 70 (Figure 5) is the only area we mapped the fault as visible in the lidar data (well-constrained and/or moderately-constrained). To the northeast, the DWF is buried by Holocene Sevier River fluvial deposits. This buried fault forms the western escarpment of a series of low hills between Joseph and Monroe (Figure 5). Most of this fault zone is buried by young Holocene and Pleistocene deposits, and we found no evidence of younger surface fault rupture on the DWF and the Quaternary age category is appropriate for this fault.

Marysvale-Circleville Area Faults

The Marysvale-Circleville area faults consist of numerous, discontinuous, complex zones of both east- and west-dipping fault scarps around the rural towns of Circleville and Marysvale. These faults were previously named the Sevier Valley-Marysvale-Circleville area faults and the Sevier Valley fault (Hecker, 1993) To avoid confusion and simplify fault naming, we have grouped these and given them the name Marysvale-Circleville area faults (MCF).

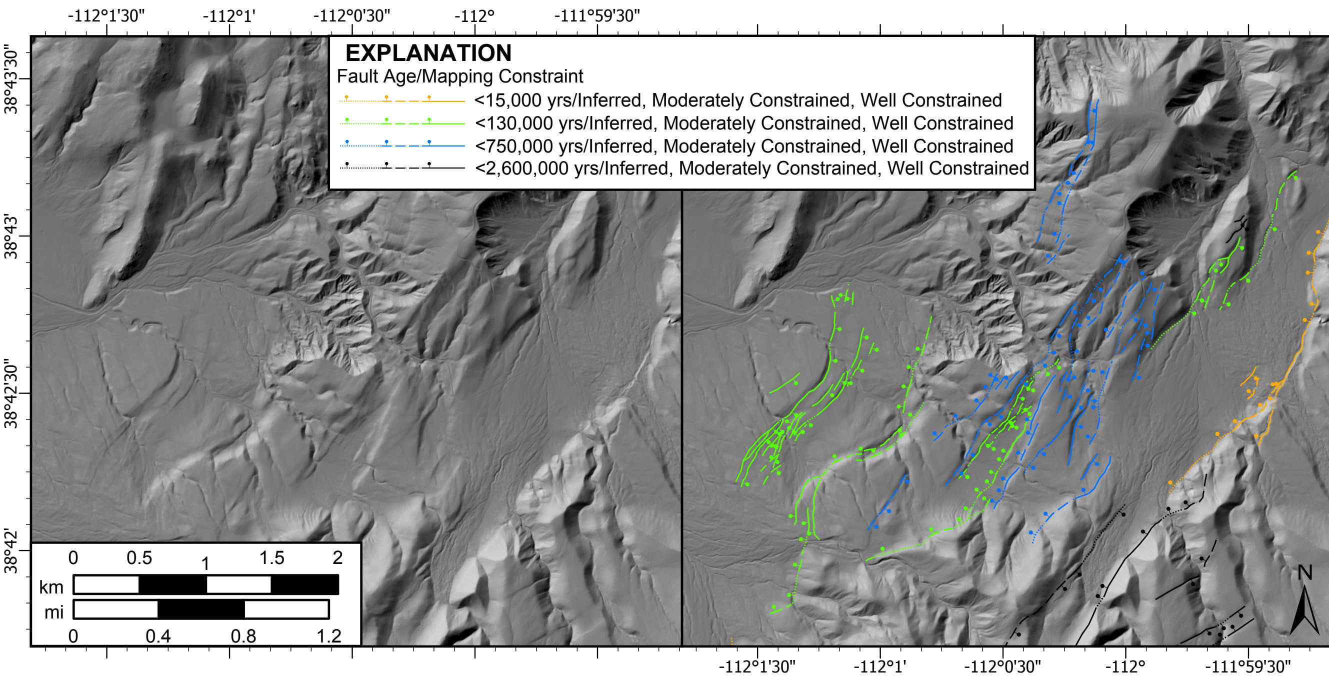

Figure 13. *Hillshade images of the Annabella Graben. Basemap from USGS 3DEP program. The right image shows fault trace mapping from this study.*

This naming convention follows the original name given to the MCF by Anderson and Bucknam (1979).

The Marysvale Volcanic Field, one of the largest Tertiary eruptive edifices in the western U.S. (Rowley et al., 1988a, 1998, in review; Biek et al., 2015, 2023), is located in the immediate area around the MCF. This large volcanic field is more than 60 miles (100 km) in diameter (Rowley et al., 1979a), consists mainly of a large volcanic accumulation which is more than 100 km in diameter, and covers much of the region around Marysvale and Circleville (Rowley et al., 1979a).

The faults of the MCF exhibit a highly discontinuous pattern and generally form in discrete clusters (Figure 6). Age estimates for scarps associated with the MCF range from Quaternary to Holocene, as many of these scarps cut alluvial fans of various ages. Anderson (1986) interpreted many of these zones of discontinuous faults as associated with the Marysvale Volcanic Field or mass wasting. However, due to the geomorphic sharpness and young apparent age of most of them, we speculate they are indeed seismogenic, not associated with volcanics in the area, and classify them as Class A faults.

Directly northwest of the town of Circleville, a complex zone of faulting (Figure 6) has several subtle fault scarps cutting Holocene-age alluvial fans. Anderson and Rowley (1986) mapped several Quaternary-age fault scarps on the Circleville 7.5-minute geologic map in this same area, but did not identify any Holocene-age scarps. However, they mention mapping several small lineaments that could possibly represent subtle fault scarps cutting Holocene-age deposits that match our newer, lidar-based mapping. We identified several sites for paleoseismic trenching on these younger fault scarps.

Near the town of Marysvale, ~2.5 miles (4 km) east of the Tushar Mountains range front, several complex zones of east- and west-dipping fault scarps form a large graben on late Quaternary fan surfaces. Farther south, this zone of faulting becomes more complex near the town of Circleville. Several well-preserved scarps are formed on Middle to Late Holocene alluvial fans, suggesting recent surface rupture (Anderson and Rowley, 1986).

On the southeast side of Piute Reservoir, we mapped numerous scarps formed on late-Quaternary alluvial fan surfaces. These scarps trend directly towards Piute Reservoir dam. One of these faults was studied by Simon Bymaster Inc. (2001) as part of a dam-site suitability study. This geotechnical study included several paleoseismic trenches. Data from these trenches showed evidence for at least two paleoearthquakes, with the most recent event occurring approximately 8000 years ago, and the penultimate event occurring approximately 14,000 to 18,000 years ago. Using data from Bymaster Inc. (2001), we have applied the <15 ka age category for one fault trace near Piute Reservoir dam (Figure 6). This geotechnical study represents the only paleoseismic information available for any of the MCF faults.

Several sites for paleoseismic trenching were identified along the MCF. However, due to the distributed nature of faulting, numerous paleoseismic trenches would be needed to recover the entire paleoseismic history of faults in this area. The one study conducted near Piute Reservoir (Simon Bymaster Inc., 2001) yielding a Holocene age is very intriguing and raises the possibility that the MCF is more recently active than previously thought, which additional paleoseismic studies would help to address.

Tushar Mountains (East Side) Fault

The Tushar Mountains (East Side) fault bounds the eastern margin of the Tushar Mountains. This poorly understood fault is mapped as mostly concealed along the range front to the west of Marysvale with little to no expression on young alluvial fans. The assigned Quaternary age category of this fault is inferred from the linear and steep range-front morphology along the eastern escarpment of the Tushar Range, and limited surface offset on alluvial fans along the range front. We mapped several moderately located scarps cutting Qaf3 (Early Pleistocene) and QTaf (Quaternary-Tertiary) alluvial fans near the southern end of the fault zone (Rowley et al., in review). These scarps are diffuse and poorly located, but represent the only scarps formed on unconsolidated deposits along the Tushar Mountains (East Side) fault. Due to the lack of young, offset alluvial fans, we did not identify any potential paleoseismic sites on this fault.

SUMMARY

This report presents the motivation, methods, and products involved in our re-mapping of central Utah regional faults. We present detailed mapping of Quaternary faults in central Utah created using high-resolution lidar elevation data and derivative products that are published in their final form in the *Utah Geologic Hazards Portal* (Utah Geological Survey, undated) and included in an ArcGIS geodatabase with this report. We mapped these faults to the best of our professional ability. In the event of a large earthquake in the central Utah region, surface-fault-rupture may occur on a previously un-mapped or un-identified fault. The motivation for this work was timely due to the availability of the high-resolution lidar data and the increasing population growth and development, specifically in the Sevier Valley region of Utah.

Surface-fault-rupture special-study zones were created based on the certainty of the fault-trace mapping and fault geometry. The special-study area dimensions are based on the *Guidelines for Evaluating Surface-Fault-Rupture Hazards in Utah* (Lund et al., 2020). These recommended special-study zones were delineated to assist in land-use planning and regulation for local governments. We identified paleoseismic sites (Table 1) along faults to foster future paleoseismic research in areas that are being rapidly developed or lacking good earthquake timing and recurrence information.

ACKNOWLEDGMENTS

This work was partially funded by the USGS Earthquake Hazards Program, External Grants Program (award number G24AP00313) and the UGS. We thank Sofia Agopian, Emily Kleber, and Greg McDonald at UGS for thorough peer reviews of this work.

The UGS recognizes and acknowledges that the land discussed in this proposal is the traditional and ancestral homeland of the Nuwuvi (Southern Piute) and Núu-agha-tʉvʉ-pʉ̱ (Ute) people. The ancestral languages spoken in this region are the Southern Piute and Ute languages. Portions of the Kanosh Band of Paiute Indians and Koosharem Band of Paiute Indians of Utah reservations lie nearby and within the project area. This study will be provided to each of these tribal governments.

REFERENCES

Anderson, J.J., 1986, Geologic map of the Circleville Mountain quadrangle, Beaver, Piute, Iron, and Garfield Counties, Utah: Utah Geological and Mineral Survey Map 80, 6 p., 2 plates., scale 1:24,000, https://doi.org/10.34191/M-80.

Anderson, J.J., and Rowley, P.D., 1986, Geologic map of the Circleville quadrangle, Beaver, Piute, Iron, and Garfield Counties, Utah: Utah Geological Survey Map 82, 7 p., 2 plates, 1:24,000 scale, https://doi.org/10.34191/M-82.

Anderson, J.J., Rowley, P.D., Blackman, J.T., Mehnert, H.H., and Grant, T.C., 1990, Geologic map of the Circleville Canyon area, southern Tushar Mountains and northern Markagunt Plateau, Beaver, Garfield, Iron, and Piute Counties, Utah: U.S. Geological Survey Miscellaneous Investigations Series Map I-2000, 1 plate, scale 1:50,000, https://doi.org/10.3133/i2000.

Anderson, L.W., and Miller, D.G., 1979, Quaternary fault map of Utah: Long Beach, California, Fugro, Inc, 35 p. pamphlet, scale 1:500,000.

Anderson, R.E., and Barnhard, T.P., 1992, Neotectonic framework of the central Sevier Valley area, Utah, and its relationship to seismicity, *in* Gori, P.L., and Hays, W.W., editors, Assessment of regional earthquake hazards and risk along the Wasatch Front, Utah: U.S. Geological Survey Professional Paper 1500-F, 47 p., https://doi.org/10.3133/pp1500AJ.

Anderson, R.E., and Bucknam, R.C., 1979, Map of fault scarps in unconsolidated sediments, Richfield 1° x 2° quadrangle, Utah: U.S. Geological Survey Open-File Report 79-1236, 17 p., 1 plate, 1:100,000 scale, https://doi.org/10.3133/ofr791236.

Arabasz, W.J., Burlacu, R., and Pechmann, J.C., 2017, Earthquake database for Utah Geological Survey Map 277—Utah earthquakes (1850–2016) and Quaternary faults:

Utah Geological Survey Open-File Report 667, https://doi.org/10.34191/OFR-667.

Biek, R.F., Eaton, J.G., Rowley, P.D., Hacker, D.B., Mattox, S.R., Bailey, C., and Marchetti, D.W., 2023, Geologic map of the west half of the Loa 30' x 60' quadrangle, Garfield, Piute, and Wayne Counties, Utah: Utah Geological Survey Map 292DM, 42 p., 2 plates, scale 1:62,500, https://doi.org/10.34191/M-292DM.

Biek, R.F., Rowley, P.D., Anderson, J.J., Maldonado, F., Moore, D.W., Hacker, D.B., Eaton, J.G., Hereford, R., Filkorn, H.F., and Matyjasik, B., 2015, Geologic map of the Panguitch 30′ x 60′ quadrangle, Garfield, Iron, and Kane Counties, Utah: Utah Geological Survey Map 270DM, 162 p., 3 plates, scale 1:62,500, https://doi.org/10.34191/M-270DM.

Bjorklund, L.J., and Robinson, G.B., 1968, Ground-water resources of the Sevier River basin between Yuba dam and Leamington Canyon, Utah: U.S. Geological Survey Water Supply Paper 1848, 79 p., 2 plates, https://doi.org/10.3133/wsp1848.

Black, B.D., Hecker, S., Hylland, M.D., Christensen, G.E., and McDonald, G.N., 2003, Quaternary fault and fold database and map of Utah: Utah Geological Survey Map M-193DM, 23 p., 1 plate, scale 1:500,000, https://doi.org/10.34191/M-193dm.

Bryant, W.A., and Hart, E.W., 2007, Fault-rupture hazard zones in California—Alquist-Priolo earthquake fault zoning act with index to earthquake fault zones maps: California Geological Survey Special Publication 42, 38 p., https://filelib.wildlife.ca.gov/FileLib/Ballona_Restoration_EIR_Reference_Material/3-06_GeoSoils_Refs/Hart&Bryant_1997.pdf.

Bucknam, R.C., and Anderson, R.E., 1979, Map of fault scarps on unconsolidated sediments, Delta 1° x 2° quadrangle, Utah: U.S. Geological Survey Open-File Report 79-366, 21 p., scale 1:250,000, https://doi.org/10.3133/ofr79366.

Bucknam, R.C., Crone, A.J., and Machette, M.N., 1989, Characteristics of active faults, *in* Jacobson, J.L., editors., National Earthquake Hazards Reduction Program, summaries of technical reports volume XXVIII: U.S. Geological Survey Open-File Report 89-453, p. 117, https://doi.org/10.3133/ofr89453.

Clark, D.L., 1990, Provisional geologic map of the Juab Quadrangle, Juab County, Utah: Utah Geological Survey Map 132, 18 p., 2 plates, 1:24,000 scale, https://doi.org/10.34191/M-132.

Clark, D.L., 2003, Geologic map of the Sage Valley 7.5′ quadrangle, Juab County, Utah: Utah Geological Survey Miscellaneous Publication 03-2, 57 p., 2 plates, 1:24,000 scale, https://doi.org/10.34191/MP-03-2.

Crone, A.J., and Wheeler, R.L., 2000, Data for Quaternary faults, liquefaction features, and possible tectonic features in the central and eastern United States, east of the Rocky Mountain front: U.S. Geological Survey Open-File Report 00-260, 342 p.

Cunningham, C.G., Steven, T.A., Rowley, P.D., Glassgold, L.B., and Anderson, J.J., 1983, Geologic map of the Tushar Mountains and adjoining areas, Marysvale volcanic field, Utah: U.S. Geological Survey Miscellaneous Investigations Series Map I-1430-A, 1:50,000 scale, https://doi.org/10.3133/i2645A.

Farm Service Agency, Commodity Stabilization Service (CSS), 1953–1961, Aerial photography sets, Sevier County, Utah: https://imagery.geology.utah.gov/pages/search.php?search=%21collection499.

Felger, T.J., Clark, D.L., and Hylland, M.D., 2007, Geologic map of the Skinner Peaks quadrangle, Juab and Sanpete Counties, Utah: Utah Geological Survey Map 223, 2 plates, 1:24,000 scale, https://doi.org/10.34191/M-223.

Gerhart Consultants Incorporated, 2003, Sevier Bridge dam site conditions, Sevier County, Utah: unpublished consultant's report, 27 p., https://geodata.geology.utah.gov/pages/download.php?direct=1&noattach=true&ref=35380&ext=pdf&k=.

Griswold, D.H., 1948, Location of inferred fracture zone and reported depths to ground water in lower Round Valley near Scipio: U.S. Soil Conservation Service unpublished map and memo, 2 p., 1 plate, https://geodata.geology.utah.gov/pages/download.php?direct=1&noattach=true&ref=3592&ext=pdf&k=.

Haller, K.M., Machette, M.N., and Dart, R.L., 1993, Maps of major active faults, western hemisphere—International lithosphere program (ILP), Project II-2—Guidelines for U.S. database and map: U.S. Geological Survey Open-File Report 93-338, 47 p.

Hanks, T.C., Bucknam, R.C., Lajoie, K.R., and Wallace, R.E., 1984, Modification of wave-cut and faulting-controlled landforms: Journal of Geophysical Research, v. 89, no. B7, p. 5771–5790.

Hecker, S., 1993, Quaternary tectonics of Utah with emphasis on earthquake-hazard characterization: Utah Geological Survey Bulletin 127, 157 p., 6 plates, scale 1:500,000, https://doi.org/10.34191/B-127.

Heidemann, H.K., 2018, Lidar base specification (ver. 1.3, February 2018): U.S. Geological Survey Techniques and Methods, book 11, chap. B4, 101 p., http://dx.doi.org/10.3133/tm11B4.

Hintze, L.F., 1991a, Interim geologic map of the Scipio Lake quadrangle, Millard County, Utah: Utah Geological Survey Open-File Report 228, 1 plate, 1:24,000 scale, https://doi.org/10.34191/OFR-228.

Hintze, L.F., 1991b, Interim geologic map of the Scipio South quadrangle, Millard County, Utah: Utah Geological Survey Open-File Report 218, 1 plate, 1:24,000 scale, https://doi.org/10.34191/OFR-218.

Hintze, L.F., 1991c, Interim geologic map of the Williams Peak quadrangle, Millard County, Utah: Utah Geological Survey Open-File Report 223, 1 plate, 1:24,000 scale, https://doi.org/10.34191/OFR-223.

Hintze, L.F., 1991d, Interim geologic map of the Scipio North quadrangle, Millard County, Utah: Utah Geological Survey Open-File Report 219, 1 plate, 1:24,000 scale, https://doi.org/10.34191/OFR-219.

Hintze, L.F., 1991e, Interim geologic map of the Fool Creek Peak quadrangle, Millard County, Utah: Utah Geological Survey Open-File Report 220, 1 plate, 1:24,000 scale, https://doi.org/10.34191/OFR-220.

Hintze, L.F., and Davis, F.D., 2002, Geologic map of the Delta 30' x 60' quadrangle and part of the Lynndyl 30′ x 60′ quadrangle, northeast Millard County, and parts of Juab, Sanpete, and Sevier Counties, Utah: Utah Geological Survey Map 206DM, 2 plates, scale 1:100,000, https://doi.org/10.34191/M-206dm.

Hintze, L.F., Davis, F.D., Rowley, P.D., Cunningham, C.G., Steven, T.A., and Willis, G.C., 2008, Geologic map of the Richfield 30' x 60' quadrangle, southeast Millard County and parts of Beaver, Piute, and Sevier Counties, Utah: Utah Geological Survey Map 195DM, 2 plates, scale 1:100,000, https://doi.org/10.34191/M-195dm.

Hiscock, A.I., and Hylland, M.D., 2015, Surface fault rupture hazard maps of the Levan and Fayette segments of the Wasatch fault zone, Juab and Sanpete Counties, Utah: Utah Geological Survey Open-File Report 640, 7 plates, scale 1:24,000, https://doi.org/10.34191/OFR-640.

Hiscock, A.I., Kleber, E.J., Jänecke, S.U., McDonald, G.N., Oaks, R.Q., Jr., and Rittenour, T., 2024, Fault trace mapping and surface-fault-rupture special study zone delineation of the East and West Cache fault zones and other regional faults, Utah: Utah Geological Survey Report of Investigation 286, 27 p., 1 appendix, https://doi.org/10.34191/RI-286.

Hiscock, A.I., Lifton, Z.M., McDonald, G.N., and Kleber, E.J., 2021, Detailed mapping of the east and west Bear Lake fault zones, Utah and Idaho, and the Oquirrh, Southern Oquirrh Mountains, Topliff Hills, and Rush Valley fault zones, Utah—Using new high-resolution lidar data to reduce earthquake risk: Final Technical Report to the U.S. Geological Survey, National Earthquake Hazards Reduction Program, award nos. G19AP00072 and G19AP00073, 35 p., https://geodata.geology.utah.gov/pages/view.php?ref=65364.

Hylland, M.D., and Machette, M.N., 2008, Surficial geologic map of the Levan and Fayette segments of the Wasatch fault zone, Juab and Sanpete Counties, Utah: Utah Geological Survey Map 229, 37 p., 1 plate, scale 1:50,000, https://doi.org/10.34191/M-229.

Knudsen, T.R., Hiscock, A.I., Ben-Horin, J., and Pearthree, P.A., 2021, Detailed mapping of the Washington, Hurricane, and Sevier/Toroweap fault zones, Utah and Arizona—Using new high-resolution lidar data to reduce earthquake risk: Final Technical Report to the U.S. Geological Survey, National Earthquake Hazards Reduction Program, award nos. G20AP0007 and G20AP0008, 36 p., https://geodata.geology.utah.gov/pages/view.php?ref=65953.

Lund, W.R., Christenson, G.E., Batatian, L.D., and Nelson, C.V., 2020, Guidelines for evaluating surface-fault-rupture hazards in Utah, *in* Bowman, S.D., and Lund, W.R., editors, Guidelines for investigating geologic hazards and preparing engineering-geology reports, with a suggested approach to geologic-hazard ordinances in Utah, second edition: Utah Geological Survey Circular 128, p. 31–58, https://doi.org/10.34191/C-128.

McDonald, G.N., Hiscock, A.I., and Hylland, M.D., 2019, Paleoseismic investigation of the Levan and Fayette segments of the Wasatch fault zone, Juab and Sanpete Counties, Utah: Utah Geological Survey, Final Technical Report to the U.S. Geological Survey, Earthquake Hazards External Grants Program, award no. G17AP00060.

McDonald, G.N., Kleber, E.J., Hiscock, A.I., Bennett, S.E.K., and Bowman, S.D., 2020, Fault trace mapping and surface-fault-rupture special study zone delineation of the Wasatch fault zone, Utah and Idaho: Utah Geological Survey Report of Investigation 280, 23 p., https://doi.org/10.34191/RI-280.

Meigs, A., 2013, Active tectonics and the LiDAR revolution: Lithosphere, v. 5, no. 2, p. 226–229.

Michaels, R.B., 1994, Geologic map of the Scipio Pass quadrangle, Millard County, Utah: Utah Geological Survey Map 164, 28 p., 2 plates, 1:24,000 scale, https://doi.org/10.34191/M-164.

Oviatt, C.G., 1992, Quaternary geology of the Scipio Valley area, Millard and Juab Counties, Utah: Utah Geological Survey Special Studies 79, 16 p., scale 1:100,000, https://doi.org/10.34191/SS-79.

Oviatt, C.G., and Hintze, L.F., 2005, Interim geologic map of the Mills quadrangle, Juab County, Utah: Utah Geological Survey Open-File Report 445, 6 p., 1 plate, 1:24,000 scale, https://doi.org/10.34191/OFR-445.

Perlich, P.S., Hollingshaus, M., Harris, E.R., Tennert, J., and Hogue, M.T., 2017, Utah's long-term demographic and economic projections summary: University of Utah Kem C. Gardner Policy Institute, 32 p.

Peterson, D.H., 1997, Geologic map of the Hayes Canyon quadrangle, Sanpete County, Utah: Utah Geological Survey Miscellaneous Publication 97-3, 20 p., 2 plates, 1:24,000 scale, https://doi.org/10.34191/MP-97-3.

Rowley, P.D., Biek, R.F., Hacker, D.B., Vice, G.S., McDonald, R.E., Maxwell, D.J., Fasselin, R., Dustin, J., Cunningham, C.G., Steven, T.A., Anderson, J.J., Ekren, E.B., Machette, M.N., Wardlaw, B.R., Smith, Z.D., Kirby, S.M., Knudsen, T.R., Kleber, E.J., Hiscock, A.I., Malone, D.H., Rivera, T.A., and Jicha, B.R., in review, Geologic map of the Beaver 30' x 60' quadrangle, Beaver, Piute, Iron, and Garfield Counties, Utah: Utah Geological Survey Map, 2 plates, scale 1:62,500.

Rowley, P.D., Cunningham, C.G., Anderson, J.J., and Steven, T.A., 1979b, Geologic map of the Marysvale SW quadrangle, Piute County, Utah: U.S. Geological Survey Miscellaneous Field Studies Map 1116, 1 plate, 1:24,000 scale, https://doi.org/10.3133/mf1116.

Rowley, P.D., Cunningham, C.G., and Kaplan, A.M., 1981a, Geologic map of the Monroe SE quadrangle, Sevier and Piute Counties, Utah: U.S. Geological Survey Miscellaneous Field Studies Map 1331, 1 plate, 1:24,000 scale, https://doi.org/10.3133/mf1331.

Rowley, P.D., Cunningham, C.G., Steven, T.A., Mehnert, H.H., and Naeser, C.W., 1988a, Geologic map of the Marysvale quadrangle, Piute County, Utah: Utah Geological Survey Map 105, 17 p., 2 plates, 1:24,000 scale, https://doi.org/10.34191/M-105.

Rowley, P.D., Cunningham, C.G., Steven, T.A., Mehnert, H.H., and Naeser, C.W., 1988b, Geologic map of the Antelope Range quadrangle, Piute County, Utah: Utah Geological Survey Map 106, 16 p., 2 plates, 1:24,000 scale, https://doi.org/10.34191/M-106.

Rowley, P.D., Cunningham, C.G., Steven, T.A., Mehnert, H.H., and Naeser, C.W., 1998, Cenozoic igneous and tectonic setting of the Marysvale volcanic field, and its relation to other igneous centers in Utah and Nevada, *in* Friedman, J.D., and Huffman, A.C., Jr., coordinators, Laccolith complexes of southeastern Utah—time of emplacement and tectonic setting—workshop proceedings: U.S. Geological Survey Bulletin 2158, p. 167–202.

Rowley, P.D., Cunningham, C.G., Steven, T.A., Workman, J.B., Anderson, J.J., and Theissen, K.M., 2002, Geologic map of the central Marysvale Volcanic Field, southwestern Utah: U.S. Geological Survey Geologic Investigations Series I-2645-A, 2 plates, 1:100,000 scale, https://doi.org/10.3133/i2645A.

Rowley, P.D., Steven, T.A., Anderson, J.J., and Cunningham, C.G., 1979a, Cenozoic stratigraphic and structural framework of southwestern Utah: U.S. Geological Survey Professional Paper 1149, 22 p., https://doi.org/10.3133/pp1149.

Rowley, P.D., Steven, T.A., and Kaplan, A.B., 1981b, Geologic map of the Monroe NE quadrangle, Sevier County, Utah: U.S. Geological Survey Miscellaneous Field Studies Map 1330, 1 plate, 1:24,000 scale, https://doi.org/10.3133/mf1330.

Rowley, P.D., Vice, G.S., McDonald, R.E., Anderson, J.J., Machette, M.N., Maxwell, D.J., Ekren, B., Cunningham, C.G., Steven, T.A., and Wardlaw, B.R., 2005, Interim geologic map of the Beaver 30' x 60' quadrangle, Beaver, Piute, Iron, and Garfield Counties, Utah: Utah Geological Survey Open-File Report 454, 28 p., 1 plate, https://doi.org/10.34191/OFR-454.

Simon Bymaster, Inc, 2001, Engineering geologic study, Piute dam and proposed relocation site, Piute County, Utah: SBI Project No. 2-01-175, November 12, 2001, https://geodata.geology.utah.gov/pages/view.php?ref=33398.

Smith, R.B., and Sbar, M.L., 1974, Contemporary seismicity in the Intermountain Seismic Belt: Geological Society of America Bulletin, v. 85, p. 1205–1218.

Standlee, L.A., 1982, Structure and stratigraphy of Jurassic rocks in central Utah—Their influence on tectonic development of the Cordilleran foreland thrust belt, *in* Powers, R.B., editor, Geologic studies of the Cordilleran thrust belt: Rocky Mountain Association of Geologists, v. 1, p. 357–382, https://archives.datapages.com/data/rmag/GeoStudCordV1_82/standlee.htm.

Stokes, W.L., 1977, Physiographic subdivisions of Utah: Utah Geological and Mineral Survey Map 43, scale 1:2,400,000, https://doi.org/10.34191/M-43.

Stokes, W.L., 1986, Geology of Utah: Salt Lake City, University of Utah Museum of Natural History and Utah Geological and Mineral Survey, 280 p., https://doi.org/10.34191/MP-S.

Steven, T.A., 1979, Geologic map of the Monroe NW quadrangle, Sevier County, Utah: U.S. Geological Survey Miscellaneous Field Studies Map 1107, 1 plate, 1:24,000 scale, https://doi.org/10.3133/mf1107.

University of Utah Seismograph Stations, 2020a, 1901 Southern Utah M 6.5±— Intermountain Seismic Belt historical earthquake project: https://quake.utah.edu/isbhep/1901-southern-utah/, accessed April 27, 2023.

University of Utah Seismograph Stations, 2020b, 1921 Elsinore, UT (series) M6±—Intermountain Seismic Belt historical earthquake project: https://quake.utah.edu/isbhep/1921-elsinore-ut/, accessed April 27, 2023.

U. S. Bureau of Land Management, 1975, Monticello-Richfield Infared Aerial Imagery: https://earthexplorer.usgs.gov/download/external/options/aerial_combin/AR4M-RIR07009021/M2M/, accessed April 2023.

U.S. Geological Survey, undated(a), Quaternary fault and fold database of the United States: https://www.usgs.gov/programs/earthquake-hazards/faults, accessed 2025.

U.S. Geological Survey, undated(b), Earthquake catalog: https://earthquake.usgs.gov/earthquakes, accessed 2025.

Utah Geological Survey, undated, Utah Geologic Hazards Portal: https://hazards.geology.utah.gov, accessed July, 2025.

Utah Geospatial Reference Center, 2016, Monroe Mountain lidar elevation data: https://gis.utah.gov/data/elevation-and-terrain/2016-lidar-monroe-mtn/, accessed April 2023.

Utah Geospatial Reference Center, 2018, Southern Utah lidar elevation data: https://gis.utah.gov/data/elevation-and-terrain/2018-lidar-southern-utah/, accessed April 2023.

Utah Geospatial Reference Center, 2020, Central and Southern Utah lidar elevation data: https://gis.utah.gov/data/elevation-and-terrain/2020-lidar-central-southern-utah/, accessed April 2023.

Wannamaker, P.E., Bartley, J.M., Sheehan, A.F., Jones C.H., Lowry, A.R., Dumitru, T.A., Ehlers, T.A., Holbrook, W.S., Farmer, G.L., Unsworth, M.J., Hall, D.B., Chapman, D.S., Okaya, D.A., John, B.E., and Wolfe, J.A., 2001, Great Basin-Colorado Plateau transition in central Utah—An interface between active extension and stable interior: Utah Geological Association Publication 30—Pacific Section, American Association of Petroleum Geologists Publication GB78, 38 p., https://archives.datapages.com/data/pacific/data/102/102001/1_ps1020001.htm.

Willis, G.C., 1988, Geologic map of the Aurora quadrangle, Sevier County, Utah: Utah Geological Survey Map 112, 25 p., 2 plates, 1:24,000 scale, https://doi.org/10.34191/M-112.

Willis, G.C., 1991, Geologic map of the Redmond Canyon quadrangle, Sanpete and Sevier Counties, Utah: Utah Geological Survey Map 138, 19 p., 2 plates, 1:24,000 scale, https://doi.org/10.34191/M-138.

Willis, G.C., 1994, Interim Geologic map of the Richfield quadrangle, Sevier County, Utah: Utah Geological Survey Open-File Report 309, 56 p., 2 plates, 1:24,000 scale, https://doi.org/10.34191/OFR-309.

Willis, G.C., Doelling, H.H., Kuehne, P.A., Marchetti, D.W., Bailey, C.M., Rowley, P.D., Higgs, K.A., Brown, K.D., and Lindgren, M.R., in review, Interim Geologic Map of the West Half of the Salina 30'x60' quadrangle, Sevier, Wayne, and Piute Counties, Utah: Utah Geological Survey Map, 56 p., 2 plates, 1:100,000 scale.

Witkind, I.J., Weiss, M.P., and Brown, T.L., 2007, Geologic map of the Manti 30' x 60' quadrangle, Carbon, Emery, Juab, Sanpete, and Sevier Counties, Utah: Utah Geological Survey Map 212DM, 2 plates, 1:100,000 scale, https://doi.org/10.34191/M-212dm.

Witkind, I.J., 1994, The role of salt on the structural development of central Utah: U.S. Geological Survey Professional Paper 1528, 145 p., https://doi.org/10.3133/pp1528.